UT TENSIO SIC VIS

MATHÉMATIQUES

Rapport Technique EP79-R-23

Classification: Library of Congress no

GENERATION OF BODY-FITTED COORDINATES FOR CASCADE COMPUTATIONS USING MULTIGRID

RICARDO CAMARERO AND MOHAMED YOUNIS

May 1979

Ecole Polytechnique de Montréal

Campus de l'Université
de Montréal
Case postale 6079
Succursale 'A'
Montréal, Québec
H3C 3A7

GENERATION OF BODY-FITTED COORDINATES FOR CASCADE COMPUTATIONS USING MULTIGRID

RICARDO CAMARERO
MOHAMED YOUNIS

MAI 1979

TABLE OF CONTENTS

page

1. INTRODUCTION..... 1

2. THE TRANSFORMATION OF COORDINATES..... 3

3. CHOICE OF A NUMERICAL SCHEME..... 6
   3.1 Discretization..... 6
   3.2 The multigrid method..... 8

4. RELAXATION SCHEMES..... 9
   4.1 Point SOR..... 9
   4.2 Line SOR..... 11
      4.2.1 SOR implicit by column..... 11
      4.2.2 SOR implicit by row..... 12
      4.2.3 Direction of relaxation sweep..... 13
   4.3 Cases studies and comparisons..... 14

5. THE MULTIGRID METHOD..... 16
   5.1 The full approximation mode of multigrid..... 16
   5.2 Correction equation for point with multigrid..... 18
   5.3 Correction equation for line SOR with multigrid..... 19
   5.4 Correction equation for row SOR with multigrid..... 19
   5.5 Applications: General considerations..... 20
   5.6 Applications: Comparisons..... 22
   5.7 Applications: Coordinate stretching..... 23

REFERENCES..... 25

ILLUSTRATIONS..... 26 to 47

ACKNOWLEDGEMENTS..... 48

1. INTRODUCTION

The governing element in the solution of a boundary value problem is the treatment of the boundary conditions. This is particularly important in numerical computations where discretization errors are introduced in the approximation of the boundaries. If these are not adequately treated, the errors arising there will spread and affect the entire computational domain. Numerous examples are available in the field of computational fluid dynamics, where such inadequate treatment of boundary conditions yield a poor solution. This is particularly frequent in practical engineering problems where complex geometries make it difficult to represent accurately the boundaries. A typical approach consists of representing a complex domain by a rectangular grid. Such an example for the type of problems investigated in this study is illustrated in Fig. 1. It is seen that near the boundaries, some grid meshes are intersected by that curve. Thus the numerical representation of these point cannot be carried out with the same scheme as for interior points. Furthermore, it is noted that the points on the boundaries rarely coincide with the nodes of the grid. This requires complicated coding to detect the various local nodal configurations and the writting of particular routines for the special treatment of such points. In addition to this, interpolation will be required, thereby increasing the discretization error.

These drawbacks can be avoided if a proper coordinate system is used. For practical problems arising from engineering applications such systems can no longer be the simple classical coordinate system. Furthermore, if the approach is to have some generality, the coordinate system must have the same degree arbitrariness as the boundaries themselves.

The intended applications of these coordinate systems is to solve fluid dynamics problems in turbomachinery applications. The essential characteristic should be that the boundaries coincide with one of the coordinate lines. These should be roughly aligned with the flow. This is particularly important when a convective computation scheme is required. An interesting feature of such coordinate systems is the adaptiveness of the grid. That is the possibility of adjusting the fineness of the discretization according to some local criteria. Finally, it is noted that the orthogonality of the system is not essential.

Such systems are called body-fitted curvilinear coordinate systems and several methods have been proposed (Ref. 1 and 2). The approach consists of solving a system of partial differential equations, which for the general conditions envisaged can only be solved numerically. The coordinate generation is the first step in the computation of a flow problem, and it is important that this step be computationaly efficient, that is a very small fraction the time required for the subsequent calculations.

This will generally depend on the numerical technique used to solve the differential equations. Ref. 1 has used a relaxation procedure whereas Ref. 2 used an A.D.I. method after introducing an artificial time. No comparison is available for these two methods. However past experience of these two method in other areas tends to favor the relaxation methods. It is easier to implement and can easily be extended to three-dimensional transformations. Furthermore, and this is the objective of this report, the convergence of relaxation schemes can be increased by at least one or two orders of magnitude by a novel technique called multigrid. This can be thought of as an acceleration of the convergence and is not too dependent on various parameters such as overrelaxation factors.

This has been applied to two basic relaxation schemes, point SOR and line SOR. Comparisons show that the computing time is reduced by factors of 2 and 3 respectively. Or the accuracy for a given computational effort is improved by one and two orders of magnitude respectively.

2. THE TRANSFORMATION OF COORDINATES

In the present study one seeks a transformation for the two-dimensional region bounded by the channel boundaris of a typical cascade as shown in Fig. 2. The characteristics of the new coordinate system is that the boundaries coincide with coordinate lines or that the channel region maps into a rectangle. One simple analogy to illustrate an extensible membrane on which a cartesian grid has been drawn. This

membrane is then streched in such a way as to make its boundaries coincide exactly with the physical region. The grid lines will be streched according to the properties of the membrane and the shape of the region it is forced to match, and the resulting grid is the sought coordinate system.

For the present application the physical coordinates (z,ϕ) is transformed into a rectangular system (η,τ) in the described manner. Mathematically, the "stretching" of the membrane is obtained by the solution of the following system of elliptic equations.

$$\alpha\phi_{\eta\eta} + \gamma\phi_{\tau\tau} - 2\beta\phi_{\eta\tau} + J^2 Q\phi_{\eta} + J^2 R\phi_{\tau} = 0 \tag{1}$$

$$\alpha Z_{\eta\eta} + \gamma Z_{\tau\tau} - 2\beta Z_{\eta\tau} + J^2 QZ_{\eta} + J^2 RZ_{\tau} = 0 \tag{2}$$

where

$$\begin{aligned} \alpha &= \phi_{\tau}^2 + Z_{\tau}^2 \\ \gamma &= \phi_{\eta}^2 + Z_{\eta}^2 \\ \beta &= \phi_{\eta}\phi_{\tau} + Z_{\eta}Z_{\tau} \\ J &= \phi_{\eta}Z_{\tau} - \phi_{\tau}Z_{\eta} \end{aligned} \tag{3}$$

This system is obtained by inverting Laplace's equation in the transformed plane. This procedure is described in Ref. 1 and 2. The four boundaries are denoted by Γ_1 Γ_2 Γ_3 and Γ_4 and coincide with $\eta = \eta_1$ for Γ_1, $\eta = \eta_2$ for Γ_2, $\tau = \tau_1$ for Γ_3 and $\tau = \tau_2$ for Γ_4. In the physical plane

$$
\begin{aligned}
\begin{pmatrix} \phi \\ Z \end{pmatrix} &= \begin{pmatrix} f_1(\eta_1, \tau) \\ f_2(\eta_1\ \tau) \end{pmatrix} \quad \text{along} \quad \Gamma_1 \\
\begin{pmatrix} \phi \\ Z \end{pmatrix} &= \begin{pmatrix} g_1(\eta_2, \tau) \\ g_2(\eta_2, \tau) \end{pmatrix} \quad \text{along} \quad \Gamma_2 \\
\begin{pmatrix} \phi \\ Z \end{pmatrix} &= \begin{pmatrix} h_1(\eta, \tau_1) \\ h_2(\eta, \tau_1) \end{pmatrix} \quad \text{along} \quad \Gamma_3 \\
\begin{pmatrix} \phi \\ Z \end{pmatrix} &= \begin{pmatrix} q_1(\eta, \tau_2) \\ q_2(\eta, \tau_2) \end{pmatrix} \quad \text{along} \quad \Gamma_4
\end{aligned}
\tag{4}
$$

The problem reduces to the solution of non-linear elliptic differential equations (1) and (2) with Dirichlet conditions on the boundary Γ. The unknowns for this problem are the physical coordinates ϕ and Z in terms of (η,τ). The imposition of the boundary conditions is to merely specify the values of the boundary shapes, i.e. values of ϕ and Z as a function of η and τ along the appropriate coordinate lines. It is noted that the correspondence of the physical points (ϕ,Z) with (η_1,τ) say along the coordinate line $\eta = \eta_1$ is arbitrary.

The functions Q and R are used to control the concentration of the coordinates lines in the physical domain. This allows the possibility of a finer discretization in certain parts of the domain where high variations of a given property is expected. In the present problem this would be the leading and trailing edges for example.

Finally it is noted that the mesh generated by the solution of (1) and (2) are not in general orthogonal and this is not essential in most problems.

3. CHOICE OF A NUMERICAL SCHEME

3.1 Discretization

The solution of the present problem is in general possible only by numerical methods. This consists of replacing the derivatives in Equations (1) and (2) by their finite difference approximations thus yielding an equivalent systems of algebraic equations. The discretization will use central differences for both first and second order derivatives yielding second order accuracy. One thus obtains for every point (η_i,τ_i) one algebraic equation for the nodal value of ϕ_{ij} and Z_{ij}. For the tangential coordinate

$$\alpha'[\phi_{i+1,j} - 2\phi_{ij} + \phi_{i-1,j}] + \gamma'[\phi_{ij+1} - 2\phi_{ij} + \phi_{ij-1}]$$
$$- 2\beta[\phi_{i+1,j+1} - \phi_{i-1,j+1} - \phi_{i+1,j-1} + \phi_{i-1,j-1}]/4\Delta\eta\Delta\tau$$
$$+ J^2Q(\phi_{i+1,j} - \phi_{i-1,j})/2\Delta\eta + J^2R[\phi_{ij+1} - \phi_{ij-1}]/2\Delta\tau = 0 \quad (5)$$

and for the axial coordinate

$$\alpha'[Z_{i+1,j} - 2Z_{ij} + Z_{i-1,j}] + \gamma'[Z_{ij+1} - 2Z_{ij} + Z_{ij-1}]$$
$$- 2\beta[Z_{i+1,j+1} - Z_{i-1,j+1} - Z_{i+1,j-1} + Z_{i-1,j-1}]/4\Delta\eta\Delta\tau$$
$$+ J^2Q(Z_{i+1,j} - Z_{i-1,j})/2\Delta\eta + J^2R[Z_{ij+1} - Z_{ij-1})/2\Delta\tau = 0 \quad (6)$$

where

$$\alpha' = ((\phi_{ij+1} - \phi_{ij-1})^2 + (Z_{ij+1} - Z_{ij-1})^2)/((2\Delta\tau)^2*(\Delta\eta)^2)$$

$$\gamma' = ((\phi_{i+1,j} - \phi_{i-1,j})^2 + (Z_{i+1,j} - Z_{i-1,j})^2)/((2\Delta\eta)^2*(\Delta\tau)^2)$$

$$\beta = ((\phi_{i+1,j} - \phi_{i-1,j})(\phi_{ij+1} - \phi_{ij-1}) + (Z_{i+1,j} - Z_{i-1,j})$$
$$(Z_{ij+1} - Z_{ij-1}))/(2\Delta\eta*2\Delta\tau) \ .$$

$$J = ((\phi_{i+1,j} - \phi_{i-1,j})(Z_{ij+1} - Z_{ij-1}) - (\phi_{ij+1} - \phi_{ij-1})(Z_{i+1,j} - Z_{i-1,j}))/(2\Delta\eta * 2\Delta\tau) \qquad (7)$$

This yields for the entire problem a system of non-linear coupled equations which must be solved iteratively, in a procedure where at each step the coefficients of Equations (5) and (6) are frozen and updated after new values of the unknowns are obtained. Essentially two approaches have been used for this class of problems

i) Successive-overrelaxation (Ref. 1).

ii) The alternating-direction-implicit schemes (Ref. 2).

In the latter approach the elliptic problem is transformed into a parabolic problem by the addition of a transient term. This can be thought of as an artificial time and each time step may be associated to an iteration of the SOR method. So both method are similar and the only criteria should be the rate of convergence, and ease of programming. No formal comparison between the two method is available and the choice was made on an intuitive basis and experience gathered by the present authors on prior application of both of these methods. It is felt that a scheme based on relaxation will yield a more efficient overall scheme.

But more importantly it is the method that lends itself best to improvements. Thus the choice of the method of solution is a successive relaxation scheme with a multigrid method to accelerate the rate of convergence.

3.2 The multigrid method

The multigrid method has been proposed by Brandt (3) and thoroughly detailled in that reference. The particular approach and software used are essentially derived from (3) and are described in detail in Ref. 4. A brief summary of the method is given here.

Examination of the rate of convergence of a classical relaxation scheme shows that an initial rapid decrease in the residual, is followed by a much slower rate of decrease. This indicates that a relaxation procedure is efficient in eliminating the frequency components of the residual which are of the same order of magniture as the mesh width. After these have been smoothed out, the remaining wavelength are slow to disappear as the scheme discretized on a given grid is not very efficient on others. This disadvantage is overcome by multigrid by carrying out the relaxation procedure on a series of grids representing the same domain. In this manner a much wider range of wavelength in the residual is eliminated thus increasing the efficiency of the method.

The particular version used is called the full approximation mode where the approximate solution on a given grid is interpolated to the need for relaxation on that grid. A particularly efficient algorithm from the computational and storage point of view has been developped (Ref. 4) and will be used in the present study.

4. RELAXATION SCHEMES

The multigrid method consists of applying any given relaxation scheme to an operator discretized on several grids. Therefore the first step in the development of the method is to devise the basic block which is the relaxation routine. Two such schemes were investigated

i) Point SOR

ii) Line SOR

4.1 Point SOR

The simplest scheme is the point SOR. The defined correction approach was used where provisional values of the variables are computed by sweeping the computational domain in a lexicographic order, say. In the calculation of these provisional values one uses corrected values and old values as illustrated in Fig. 3.

Thus Equations (5) and (6) are rewritten to solve for ϕ and Z at (i,j) surrounded by corrected and old values as shown in Fig. 3.

$$\alpha'[\phi_{i+1,j} - 2\bar{\phi}_{ij} + \phi^{+}_{i-1,j}] + \gamma'[\phi_{ij+1} - 2\bar{\phi}_{ij} + \phi^{+}_{ij-1}]$$
$$- \beta'[\phi_{i+1,j+1} - \phi_{i-1,j+1} - \phi^{+}_{i+1,j-1} + \phi^{+}_{i-1,j-1}]$$
$$+ Q'[\phi_{i+1,j} - \phi^{+}_{i-1,j}] + R'[\phi_{ij+1} - \phi^{+}_{ij-1}] = 0 \qquad (8)$$

and

$$\alpha'[Z_{i+1,j} - 2\bar{Z}_{ij} + Z^{+}_{i-1,j}] + \gamma'[Z_{ij+1} - 2\bar{Z}_{ij} + Z^{+}_{ij-1}]$$
$$- \beta'[Z_{i+1,j+1} - Z_{i-1,j+1} - Z^{+}_{i+1,j-1} + Z^{+}_{i-1,j-1}]$$
$$+ Q'[Z_{i+1,j} - Z^{+}_{i-1,j}] + R'[Z_{ij+1} - Z^{+}_{ij-1}] = 0 \qquad (9)$$

Where ϕ and Z are old values, ϕ^+ and Z^+ are corrected values, and $\bar{\phi}$ and $\bar{Z}$ are provisional values. An old value is corrected by the provisional value and a relaxation factor, ω, as follows

$$\begin{aligned} \phi^+ &= \phi + \omega(\bar{\phi}-\phi) \\ Z^+ &= Z + \omega(\bar{Z}-Z) \end{aligned} \tag{10}$$

Thus one obtains for the provisional values

$$\begin{aligned} \bar{\phi}_{ij} &= \phi_{ij} + CF_{ij}/\omega \\ \bar{Z}_{ij} &= Z_{ij} + CZ_{ij}/\omega \end{aligned} \tag{11}$$

where the corrections are defined as

$$\begin{aligned} CF_{ij} &= \phi^+_{ij} - \phi_{ij} \\ CZ_{ij} &= Z^+_{ij} - Z_{ij} \end{aligned} \tag{12}$$

Substituting Equation (11) into Equations (8) and (9) one obtains where

$$\beta' = 2\beta/4\Delta\eta\Delta\tau$$

$$Q' = J^2/2\Delta\eta$$

$$R' = J^2/2\Delta\tau$$

$$\frac{2(\alpha'+\gamma')}{\omega} CF_{ij} = RF_{ij} + (\alpha'-Q')\, CF_{i-1,j} - \beta'(Cf_{i-1,j-1} - CF_{i+1,j-1}) + (\gamma'-R')\, CF_{ij-1} \tag{13}$$

$$\frac{2(\alpha'+\gamma')}{\omega} CZ_{ij} = RZ_{ij} + (\alpha'-Q')\, CZ_{i-1,j} - \beta'(CZ_{i-1,j-1} - CZ_{i+1,j-1}) + (\gamma'-R')\, CZ_{ij-1} \tag{14}$$

where the residuals are

$$RF_{ij} = \alpha'(\phi_{i+1,j} - 2\phi_{ij} + \phi_{i-1,j}) + \gamma'(\phi_{ij+1} - 2\phi_{ij} + \phi_{ij-1}) - \beta'(\phi_{i+1,j+1} - \phi_{i-1,j+1} - \phi_{i+1,j-1} + \phi_{i-1,j-1}) + Q'(\phi_{i+1,j} - \phi_{i-1,j}) + R'(\phi_{ij+1} - \phi_{ij-1}) \tag{15}$$

$$RZ_{ij} = \alpha' \qquad \boxed{\phi \Rightarrow Z} \tag{16}$$

Thus with Equations (13) and (14) successive corrections for ϕ and Z and computed following the sweeping direction given in Fig. 3. The overall algorithm for this scheme is given in Appendix 1.

4.2 Line SOR

In line or column relaxation, all the nodes are solved implicitly at once. This yields a triadiagonal system of equations which is easily solved. Solving n points implicitly requires about the same computations as solving n times on point explicitly. The advantage lies in the fact that boundary conditions which appear as the end points of an implicit are felt immediately throughout the line, whereas, in an explicit scheme it would require about as many sweeps as there are points in the line. This makes implicit relaxation much more efficient. The correction algorithm is now described for sweeps implicit in either of the two coordinate directions.

4.2.1 SOR Implicit by column

The configuration for a typical column relaxation implicit along a τ = const coordinate line is shown in Fig. 4. The difference equations,

Equations (5) and (6) are written for the unknown points along the column taking into account, as for point relaxation, the status of the neighboring points, i.e. corrected or old.

$$\alpha'[\bar{\phi}_{i+1,j} - 2\bar{\phi}_{ij} + \bar{\phi}_{i-1,j}] + \gamma'[\phi_{i,j+1} - 2\bar{\phi}_{ij} + \phi^{+}_{ij-1}]$$
$$- \beta'[\phi_{i+1,j+1} - \phi_{i-1,j+1} - \phi^{+}_{i+1,j-1} + \phi^{+}_{i-1,j-1}]$$
$$+ Q'(\bar{\phi}_{i+1,j} - \bar{\phi}_{i-1,j}) + R'(\phi_{ij+1} - \phi^{+}_{ij-1}) = 0 \qquad (17)$$

Defining a corrected value in terms of the old and provisional values, Equations (10) and (11), one obtains the correction equations.

$$\frac{(\alpha'-Q')}{\omega} CF_{i-1,j} - \frac{2(\alpha'+\gamma')}{\omega} CF_{ij} + \frac{(\alpha'+Q')}{\omega} CF_{i+1,j}$$
$$= -RF_{ij} - \gamma' CF_{ij-1} + \beta'[CF_{i+1,j-1} - CF_{i-1,j-1}] + R' CF_{ij-1} \qquad (18)$$

$$\frac{(\alpha'-Q')}{\omega} CZ_{i-1,j} - \frac{2(\alpha'+\gamma')}{\omega} CZ_{ij} + \frac{(\alpha'+Q')}{\omega} CZ_{i+1,j}$$
$$= -RZ_{ij} - \gamma' CZ_{ij-1} + \beta'(CZ_{i+1,j-1} - CZ_{i-1,j-1}) + R' CZ_{ij-1} \qquad (19)$$

where the residuals RF_{ij} and RZ_{ij} are defined by Equations (15) and (16). Equations (18) and (19) differ from their counterpart, in point relaxation Equations (13) and (14) in that they are implicit and each equation involves three unknowns. Thus yielding a triadiagonal system.

4.2.2 SOR Implicit by row

Fig. 5 illustrates the configuration for a relaxation sweep implicit along the η = constant coordinate direction. The difference equations are written for every node along a given row and this yields,

$$\alpha'(\phi_{i+1,j} - 2\bar{\phi}_{ij} + \phi^{+}_{i-1,j}) + \gamma'(\bar{\phi}_{ij+1} - 2\bar{\phi}_{ij} + \bar{\phi}_{ij-1})$$
$$- \beta'(\phi_{i+1,j+1} - \phi^{+}_{i-1,j+1} - \phi_{i+1,j-1} + \phi^{+}_{i-1,j-1})$$
$$+ Q'(\phi_{i+1,j} - \phi^{+}_{i-1,j}) + R'(\bar{\phi}_{ij+1} - \bar{\phi}_{ij-1}) = 0 \qquad (20)$$

and
$$\alpha'[Z_{i+1,j} - 2\bar{Z}_{ij} + Z^{+}_{i-1,j}] + \gamma'[\bar{Z}_{ij+1} - 2\bar{Z}_{ij} + \bar{Z}_{ij-1}]$$
$$- \beta'[Z_{i+1,j+1} - Z^{+}_{i-1,j+1} - Z_{i+1,j-1} + Z^{+}_{i-1,j-1}]$$
$$+ Q'[Z_{i+1,j} - Z^{+}_{i-1,j}] + R'(\bar{Z}_{ij+1} - \bar{Z}_{ij-1}) = 0 \qquad (21)$$

From which as previously one obtains the correction equations

$$\frac{(\gamma'-R')}{\omega} CF_{ij-1} - \frac{(\alpha'+\gamma')}{\omega} CF_{ij} + \frac{(\gamma'+R')}{\omega} CF_{i,j+1} = -RF_{ij} - \alpha' CF_{i-1,j}$$
$$+\beta'(CF_{i-1,j+1} - CF_{i-1,j-1}$$
$$+Q'CF_{i-1,j} \qquad (22)$$

and
$$\frac{(\gamma'-R')}{\omega} CZ_{ij-1} - \frac{2(\alpha'+\gamma')}{\omega} CZ_{ij} + \frac{(\gamma'+R')}{\omega} CZ_{i,j+1} = -RZ_{ij} - \alpha' CZ_{i-1,j}$$
$$+\beta'[CZ_{i-1,j+1} - CZ_{i-1,j-1}]$$
$$+ Q'CZ_{i-1,j} \qquad (23)$$

where the residuals are defined in Equations (15) and (16).

4.2.3 Direction of relaxation sweep

For a given relaxation scheme the marching direction affects the rate of convergence. If the coefficients of the derivatives are of the same order of magnitude, then the equation will exhibit no preferred marching direction and it is best to use symmetric relaxation. In general, the marching direction should be chosen to coincide with the direction of propagation

of physical information. In this respect the boundary conditions and their types should be taken into account. The rule proposed by Brandt (3) is that every point should be relaxed either after or simultaneously with its more heavily weighted neighbors.

If such directions are not readily apparent from either the physics of the problem or when the weighting of the nodes (i.e. the coefficients) changes in the domain then sweeps should be carried out in alternating directions. This will speed up the convergence when the marching direction coincides locally with that of information propagation, and will have a neutral effect otherwise.

In the present study a line relaxation was chosen mainly to speed up the effect of the boundary conditions. Secondly as it is not known before hand how the information propagate locally, an alternating direction is chosen. This is a two-step procedure. First with a column (y) implicit scheme the entire field is relaxed marching in the positive x-direction. This is followed by a row (x) implicit relaxation marching in the positive y-direction.

4.3 Cases studies and comparisons

For the actual computations carried out in this study two typical cascades were used and are shown in figures 2a and 2b. Using the two methods described in this chapter, point and line SOR, body-fitted coordinates were obtained for these two cascades. Aside from the number of grid points, the only parameter to be varied in these calculations is the overrelaxation parameter in order to optimize the rate of convergence for the complete computation. Such evaluations were carried out by comparing the error of the solution as a function of the work units. For the present

purposes the measure of the error used is the root mean square value of the residual

$$E = \left(\Sigma R_{ij}^2 / \text{no. of points} \right)$$

and the work unit is defined as the computing time required to complete one full relaxation over the entire domain. It is noted that for the line SOR, the time required to solve the tridiagonal system was estimated to be 20% of the relaxation work.

Using point SOR, the relaxation factor was varied, between 1.0 and 1.8. The resulting relaxation histories are compared in fig. 6 and it is seen that the optimum value for this case is 1.5.

With the same cascade, this procedure was repeated with the line SOR method. The relaxation histories are compared in Fig. 7. Finally a comparison between the optimum relaxations using the point SOR and line SOR is shown in Figures 8 and 9 for the cascades shown in Figures 2a and 2b respectively. The coordinates lines are shown in Figures 10 and 11.

For these results, one can conclude that line relaxation is a more efficient technique than point relaxation. This can be explained by the fact that the former is an implicit scheme where all the points along an entire line are relaxed simultaneously. This is particularly beneficial to the relaxation process as the boundary values are felt instantaneously by the interior points.

The choice of the direction of sweep is important but was not investigated thoroughly in this study. This is presently being study using an alternating line and column relaxation and will be reported.

5. THE MULTIGRID METHOD

5.1 The full approximation mode of multigrid

The aim of this section is to apply the multigrid method to the various relaxation procedures described in section 4. The full approximation mode proposed by Brandt (3) is used with the software developed in Ref. 4. The method as applied to the present system of equations (1) and (2) is first described in general and is then specialized to point SOR, line SOR and LADSOR.

Following the notation of References 3 and 4, the system of equations (1) and (2) is denoted by the operator L.

$$L \equiv \begin{bmatrix} \alpha\phi_{\eta\eta} + \gamma\phi_{\tau\tau} - 2\beta\phi_{\eta\tau} + J^2 Q\phi_{\eta} + J^2 R\phi_{\tau} \\ \alpha Z_{\eta\eta} + \gamma Z_{\tau\tau} - 2\beta Z_{\eta\tau} + J^2 QZ_{\eta} + J^2 RZ_{\tau} \end{bmatrix} \tag{24}$$

where all coefficients are as defined in Equation (3). The associated boundary conditions are of the Dirichlet type and given by Equation (4). A hierarchy of grids ranging from the coarse, G^0 to the fine G^M will discretize the domain Γ in the (η,τ) plane. The mesh ratio, that is the ratio of a characteristic mesh size for two successive grids say $= h^k/h^{k+1}$ is set to 2. We seek numerical solutions to ϕ and Z denoted by UF and UZ that satisfy the discretized operator L on the fine grid G^M

$$L^M(UF^M, UZ^M) = 0 \tag{25}$$

The exact numerical solution UF, and UZ is approximated by uf and uz. The multigrid algorithm will compute a correction VF and VZ on each grid. These are used to correct the approximate solution. In the actual procedure, the full approximation is relaxed on each grid until it is sufficiently smooth and is then interpolated to the next grid. The relaxation sweeps are carried out with the same scheme, only the fineness of the discretization changes. The effectiveness of the multigrid method to liquidate certain frequencies corresponding to the mesh size is related to a forcing term which is added to Equation (25) on the coarser grids. This term is the difference of the residual of the operator on the fine and the current grid. Thus the "residual" equation is

$$L^K(uf^K, uz^K) = \tilde{F}^K \tag{26}$$

where

$$\tilde{F}^K = I_M^K L^M(UF^M, UZ^M) - L^K(I_M^K UF^M, I_M^K UZ^M) \tag{27}$$

The algorithm of a complete multigrid cycle is as follows"

1) An initial solution (uf^M, uz^M) is found.

2) The residual of this approximate solution is computed on G^M

$$L^M(uf^M, uz^M)$$

3) Set the parameters for G^0 and solve the residual equation

$$L^0(uf^0, uz^0) = \tilde{F}^0 \tag{28}$$

As a starting solution for this step one can use $I_\mu^0(uf^M, uz^M)$.

4) When (uf^0, uz^0) has been solved with sufficient accuracy, it is interpolated to the next grid and used as a starting solution for the next grid.

5) Set parameters for G^K

$$K = K+1$$

6) Computed the residual of (uf^M, uz^M) on G^{K+1} and obtain the forcing term

$$\tilde{F}^K = I_M^K L^M (uf^M, uz^M) - L^K (I_M^K uf^M, I_M^K uz^M) \tag{29}$$

7) Using the solution from the previous step as a starting point solve

$$L^K (uf^K, uz^K) = \tilde{F}^K \tag{30}$$

8) When (uf^K, uz^K) has been obtained with sufficient accuracy, it is interpolated to the next grid.

9) Repeat steps 5) to 8).

5.2 Correction equation for point with multigrid

The correction equation for point SOR is now modified to account for the forcing term $\tilde{F}$, equation (27). This is carried out following the same steps as in section 4.1 with $\tilde{F}$ on the right hand side of Equations (8) and (9). It is noted that the step size, $\Delta\eta$ and $\Delta\tau$ now depends on the grid. These become

$$\frac{2(\alpha'+\gamma')}{\omega} CF_{ij} = RF_{ij} - FF_{ij} + (\alpha'-Q')\, CF_{i-1,j} - \beta'(CF_{i-1,j-1} - CF_{i+1,j-1}) + (\gamma'-R')\, CF_{ij-1} \tag{31}$$

$$\frac{2(\alpha'+\gamma')}{\omega} CZ_{ij} = RZ_{ij} - FZ_{ij} + (\alpha'-Q')\, CZ_{i-1,j} - \beta'(CZ_{i-1,j} - CZ_{i+1,j-1}) + (\gamma'-R')\, CF_{ij-1} \tag{32}$$

where
$$FF_{ij} = -I_M^K L^M (UF^M) + L^K (I_M^K UF^M) \tag{33}$$

$$FZ_{ij} = -I_M^K L^M (UZ^M) + L^K (I_M^K UZ^M) \tag{34}$$

5.3 Correction equation for line SOR with multigrid

Similarly, the correction equations (18) and (19) become after the addition of the forcing term,

$$\frac{(\alpha'-Q')}{\omega} CF_{i-1,j} - \frac{2(\alpha'+\gamma')}{\omega} CF_{ij} + \frac{(\alpha'+Q')}{\omega} CF_{i+1,j}$$
$$= FF_{ij} - RF_{ij} - \gamma' CF_{ij-1}$$
$$+ \beta'(CF_{i+1,j-1} - CF_{i-1,j-1})$$
$$+ R' CF_{ij-1} \tag{35}$$

$$\frac{(\alpha'-Q')}{\omega} CZ_{i-1,j} - \frac{2(\alpha'+\gamma')}{\omega} CZ_{ij} + \frac{(\alpha'+Q')}{\omega} CZ_{i+1,j}$$
$$= FZ_{ij} - RZ_{ij} - \gamma' CZ_{ij-1}$$
$$+ \beta'(CF_{i+1,j-1} - CF_{i-1,j-1})$$
$$+ R' CZ_{ij-1} \tag{36}$$

5.4 Correction equation for row SOR with multigrid

The correction equations for row SOR equations (22) and (23) become

$$\frac{(\gamma'-R')}{\omega} CF_{ij-1} - \frac{2(\alpha'+\gamma')}{\omega} CF_{ij} + \frac{(\gamma'+R')}{\omega} CF_{i,j+1}$$
$$= FF_{ij} - RF_{ij} - \alpha' CF_{i-1,j}$$
$$+ \beta'(CF_{i-1,j+1} - CF_{i-1,j-1})$$
$$+ Q' CF_{i-1,j} \tag{37}$$

$$\frac{(\gamma'-R')}{\omega} CZ_{ij-1} - \frac{2(\alpha'+\gamma')}{\omega} CZ_{ij} + \frac{(\gamma'+R')}{\omega} CZ_{i+1,j}$$

$$= FZ_{ij} - RZ_{ij} - \alpha' CZ_{i-1,j}$$

$$+ \beta'(CZ_{i-1,j+1} - CZ_{i-1,j-1})$$

$$+ Q' CZ_{i-1,j} \qquad (38)$$

5.5 Applications: General considerations

In applying and in developing a computer program to the solution of differential equations of the type presented in this report there are several parameters that can be varied. These are related to the multigrid method and are the number of grid levels, the number of relaxation sweeps on each, and the overrelaxation factor. The effect of these parameters on the convergence of the solution is problem dependent and this is best assessed by an empirical approach based on computational experiments. This was carried out in the present paper for the elliptic equations (1) and (2) using the multigrid algorithm described in the present section and Ref. (4).

Number of grid levels

The number of grid levels available in a given computation is constrainded by the number of nodes of the discretization, the mesh ratio of the multigrid technique, and the interpolation procedure. For ease of programming, the interpolation in this study restricts the number of intervals to a multiple of the mesh ratio. This in turn, although arbitrary in principle, was chosen to be 2 or 3 and only the first value was actually used. So that the number of grid levels available is obtained

by dividing evenly the number of intervals by some power of the mesh ratio. It is suggested that this number be chosen beforehand and then the number of nodes set accordingly. In practical terms this means that for a 17×33 mesh one is restricted to a maximum of 5 grid levels. This in fact was found to be sufficient. Fig. 12 shows the relaxation histories for the solution of the coordinate on cascade A using multigrid with line relaxation. The computations were carried out with one, three and four grid levels. The comparison indicates little difference between three and four levels and suggests that there would be little advantage in using more levels.

Number of sweeps

Ideally, the number of sweeps on each grid should be chosen so that the residual equation is solved with sufficient accuracy. In practice this required an elaborate stopping criteria which in the end is also problem dependent. To avoid this, it was decided to set the number of sweeps equal for all grids and to find what this number should be.

The objective of this is an attempt to establish some general values for what could be termed an "optimum" strategy for the interplay between the coarse grid corrections and the smoothing on the fine grid.

It is emphasized that during the course of experimentation with multigrid, numerous trials were carried out using an interactive program allowing great flexibility and control over the relaxation procedure and it was found that varying the number of sweep on each grid had little effect on the overall convergence. This is illustrated in Fig. 13 showing the relaxation histories with 3, 5, 4 and 3 sweeps, 4, 3, 3 and 3 sweeps, and 3, 3, 3 and 3 sweeps on the fine to coarse grids respectively.

Therefore, it remains to find the optimum number of sweeps. For multigrid with point relaxation this was found to be 3 as illustrated in fig. 14, whereas for multigrid with line relaxation this was found to be 4, fig. 15. In fact the important factor is the number of sweeps on the fine grid, where a smooth solution is essential because it is interpolated to the coarser grid. This controls the coarse grid corrections and hence the benefits of multigrid. This is illustrated in fig. 16, where the sweeps on the fine grid were 1 and 4.

The overrelaxation factor was varied and again this was found to have no noticible effect on the overall history. This can be explained as follows. An overrelaxation factor greater than one has an important effect when the solution is smooth. Usually in the initial iterations a value of $\omega = 1.0$ gives better results, and this is precisely how multigrid works. Only a few iterations are carried out on each grid, and then the computation proceeds to the next, and thus the beneficial effect of ω would not be realized.

5.6 Applications: Comparisons

Having found the appropriate values of the pertinent parameters for the multigrid method as applied to the problem of coordinate grid generations, it remains to compare this method with the ordinary relaxation. This was done for the cascade of fig. 2a with four grid levels. The computations were carried out with the four methods described in this paper, point SOR, line SOR, multigrid with point relaxation, and multigrid with line relaxation. And each of these used the optimum parameters and

factors as determined in sections 4.3 and 5.5. The comparisons of these results are illustrated in fig. 17 for 9 × 17 grid points, fig. 18 for 17 × 33 grid points and fig. 19 for 17 × 65. In all instances the order of increasing performance is from point SOR, line SORE, multigrid with point relaxation and finally multigrid with line relaxation. So that it can be concluded that multigrid with line relaxation is the best of all four methods investigated.

Furthermore examination of these three figures, reveals an interesting feature of multigrid. The level of lowest error or residual reached in these computations depends on the number of nodes, and this is expected as this represents the fineness of the discretization. This improvement is roughly one order of magnitude every time the number of points are doubled. But the remarkable aspect is that this level of accuracy is reached with much less work for the finer meshes. For example, this level of accuracy at the R.M.S. value of 10^{-8}, requires 31 W.U. for 153 nodes, 21 W.U. for 561 nodes and 13 W.U. for 1105 nodes. Thus a fine grids can be solved more economically on an absolute basis as well as on a relative (per node) basis. This is best summarized in Fig. 20 where the optimum multigrid line relaxation are.

5.7 Applications: Coordinate stretching

One of the basic characteristics of the coordinate transformation described in this report is the possibility of stretching the grid by introducing a forcing function in the Poisson equation of chapter 2. These are the terms Q and R which act on the η and τ coordinate lines respectively. In the computations shown in sections 4.3, 5.5 and 5.6 these terms were set identically equal to zero. In this section

these will be used to concentrate coordinate lines in a given region either towards a boundary or a point. Typically these could be the cascade boundary or a the leading or trailing edges.

The form of the forcing functions Q and R can be quite general. A form which lends itself to a good physical interpretation has been proposed by Ref. 1. It is as follows. To attract η-lines to a given y_i line,

$$Q = -A \, \mathrm{sgn}(\eta-\eta_i) \, \exp\left[-B|\eta-\eta_i|\right]$$

This involves the use of two parameters A and B which can be interpreted as the strength and the range of the attraction respectively A similar expression can be written for R where the variable η is replaced by τ. To attract η-lines towards a given point (η_i,τ_i)

$$Q = -A \, \mathrm{sgn}(\eta-\eta_i) \, \exp\left(-B\sqrt{(\tau-\tau_i)^2 + (\eta-\eta_i)^2}\right)$$

The parameters are interpreted as for the previous expression. Similarly one can write a forcing function for R to attract τ lines.

The coordinate grid is very sensitive to the choice of these values. Figures 21 to 24 show coordinate grids with attraction to the bottom ($\eta = 0$) and to the top boundary ($\eta = 1$). The strength coefficient A has been set to 150 and the decay factor B has been varied from .51 and .53 in figures 22 and 23. In figure 24, two distinct values of A for the bottom (100) and for the top (200) boundaries have been chosen. Figure 21 shows the grid without attraction for comparison.

Figures 25 to 28 illustrate the attraction to the leading edge on the top boundary (η = 1, τ = leading edge) and to the trailing edge on the bottom boundary (η = 0, τ = t.e.). The strength was set to 20 for both points and the decay factor was .2, .14, .13 and .10.

The results obtained with the forcing functions were extremely sensitive to the values of the parameters. To complicate things further these depend very much on the particular problem. Under such circumstances it is essential to have at one's disposal an interactive graphics display, in order to assess the resulting grid.

REFERENCES

1. Thomson, J.F., Thames, F.C. and Mastin, W. "Automatic Numerical Generation of Body-Fitted Curvilinear Coordinate System for Field Containing any Number of Arbitrary 2-D Bodies", Journal of Computational Physics, Vol. 15 (1974), pp. 299-319.

2. Ghia, U. and Ghia, K.N. "Numerical Generation of a System of Curvilinear Coordinates for Turbine Cascade Flow Analysis", University of Cincinnati, Report #AFL75-4-17, April 1975.

3. Brandt, A. "Multi-Level Adaptive Techniques - The Multigrid Method", IBM Research Report, RC 6026, 1976.

4. Camarero, R. "A Software Package for the Multigrid Method", Ecole Polytechnique, Montreal, Rapport Technique EP79-R, February 1979.

5. Camarero, R. and Younis, M. "Generation of Body-Fitted Coordinates for Turbines Cascades Using Multigrid", Proceeding of I.S.A.B.E. IV, April 1-6, 1979, Orlando, Florida.

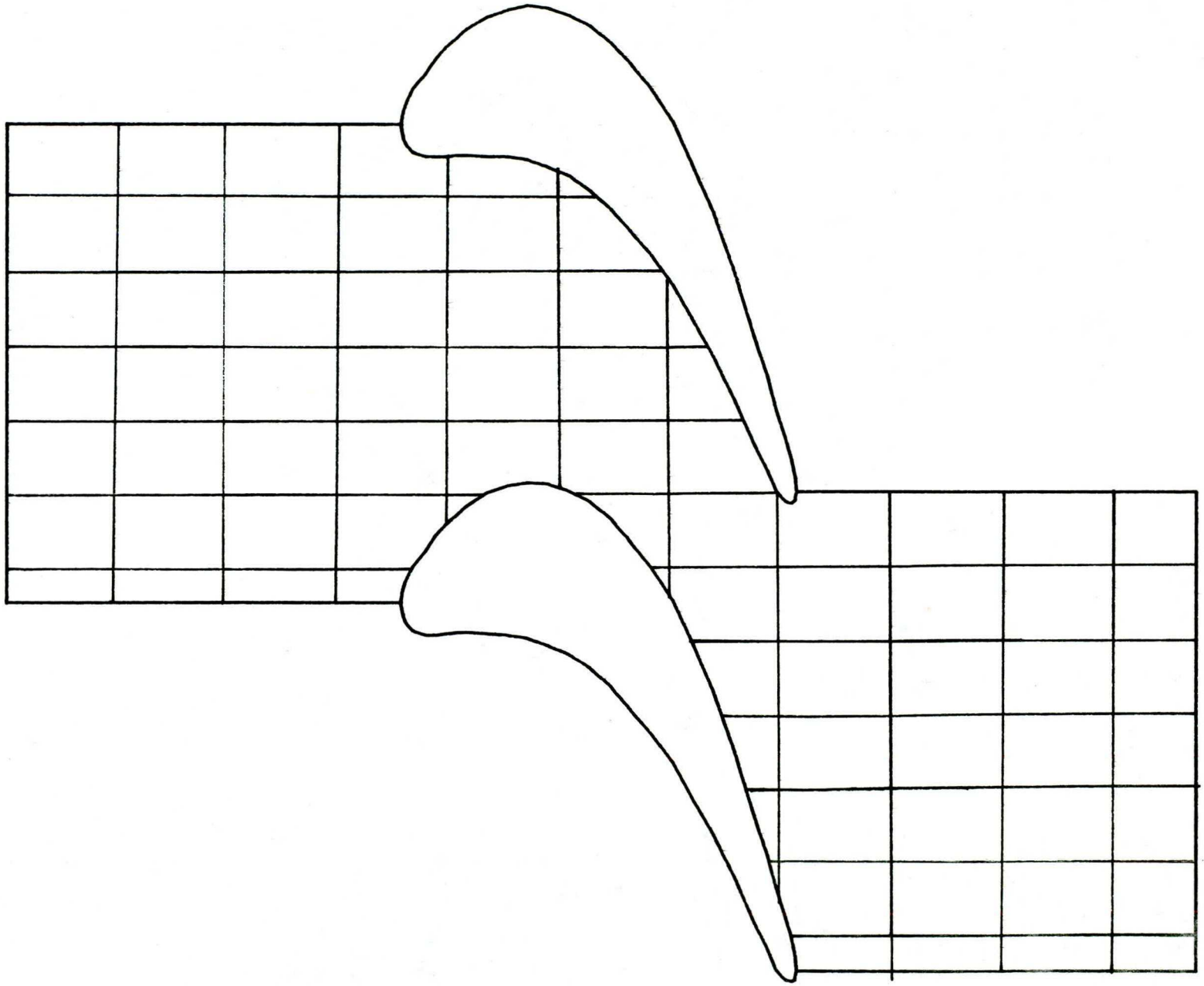

FIG. 1 RECTANGULAR GRID IN PHYSICAL COORDINATES FOR A TYPICAL CASCADE.

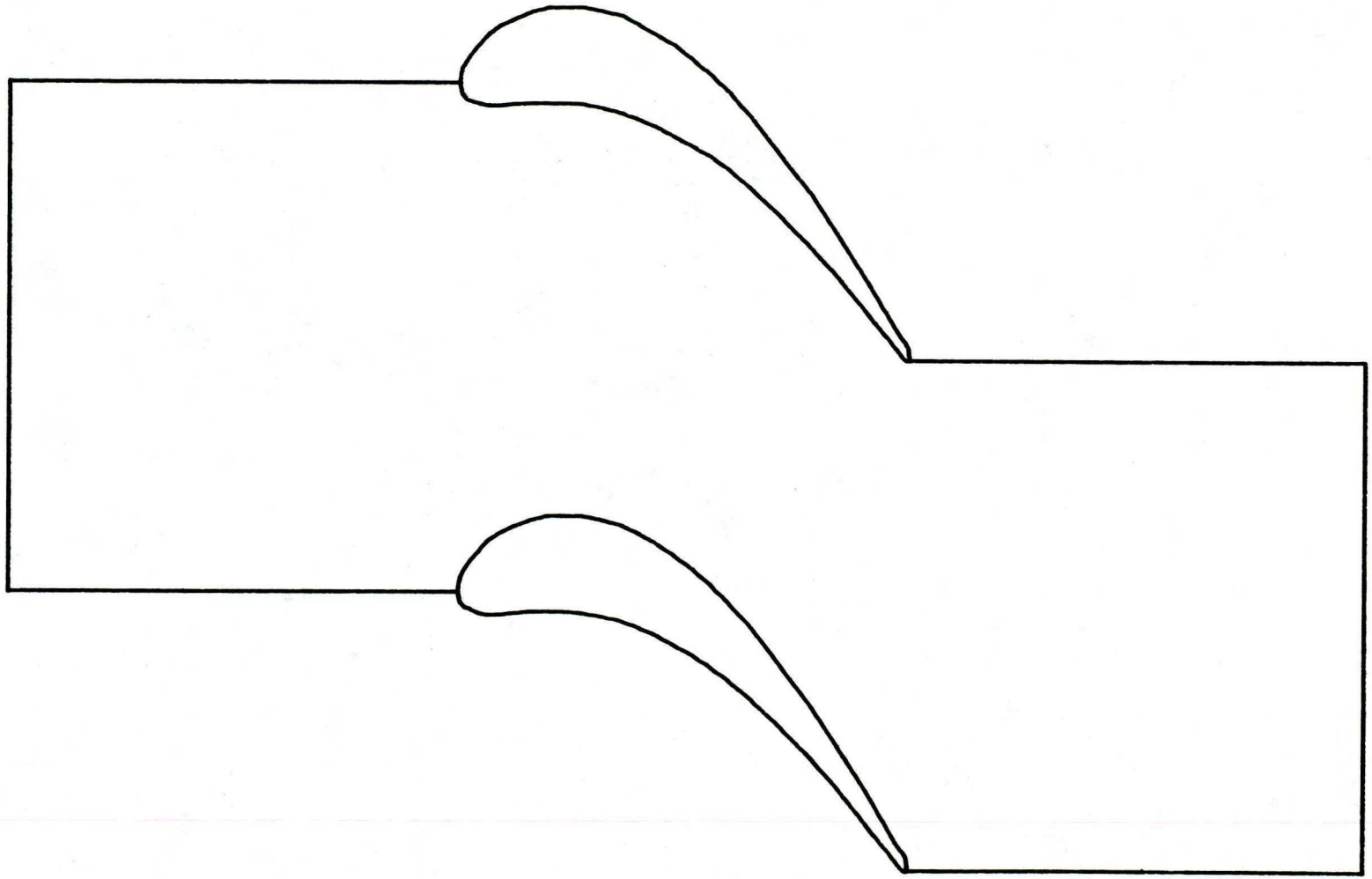

FIG. 2A CASCADE A

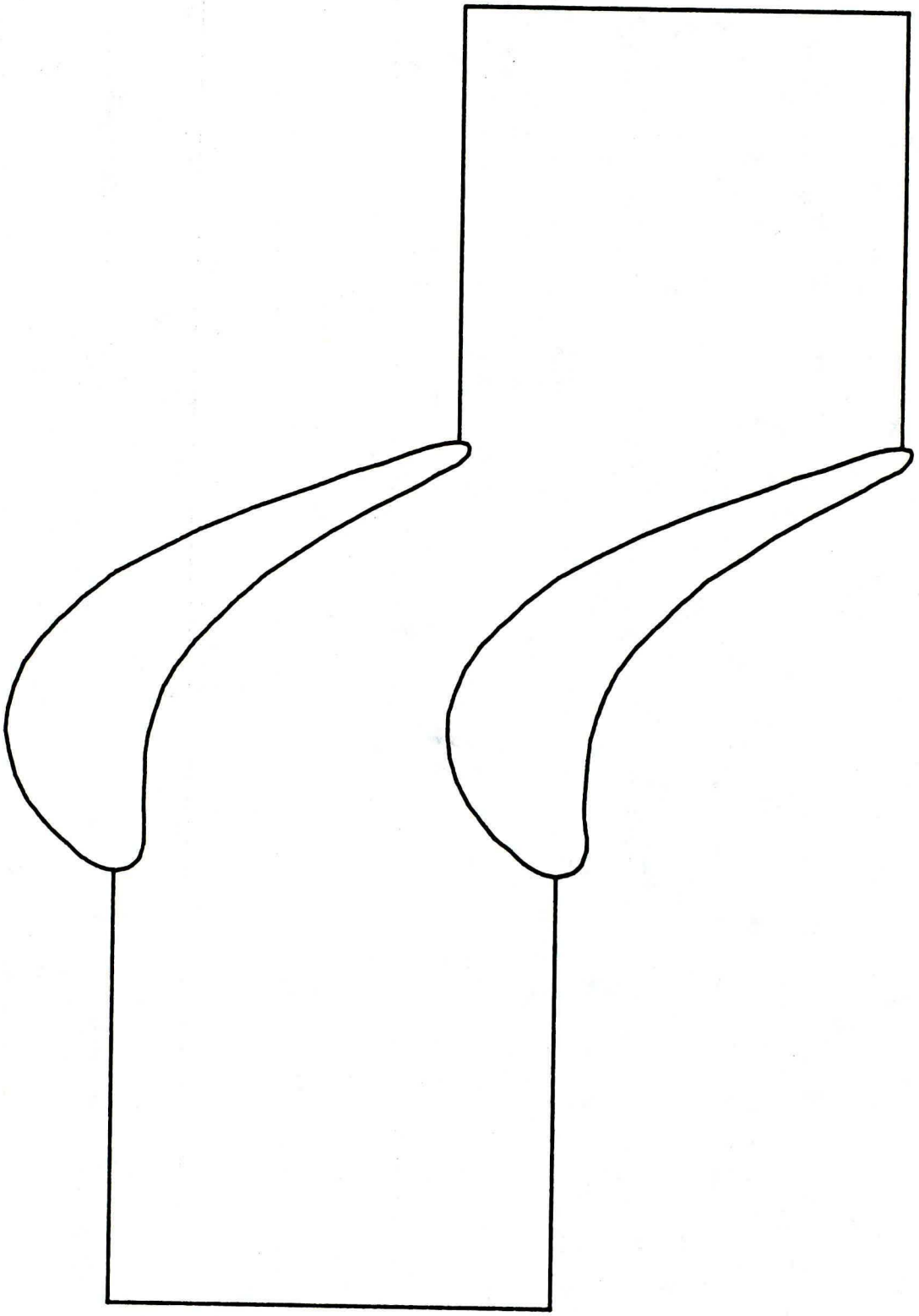

FIG. 2B CASCADE B

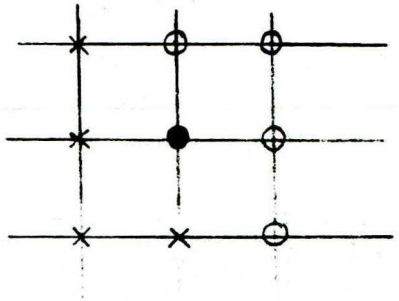

FIG. 3
POINT RELAXATION

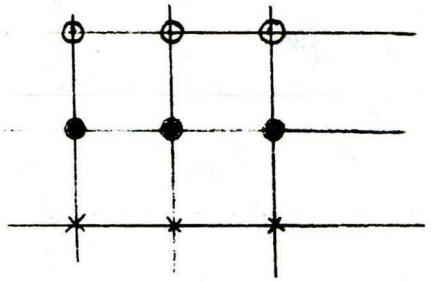

FIG. 4
LINE RELAXATION BY ROW

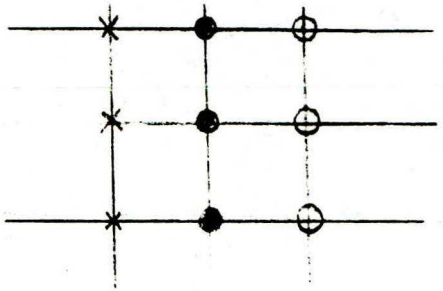

FIG. 5
LINE RELAXATION BY COLUMN

LEGEND:

X Corrected values

● Provisional values

○ Old values

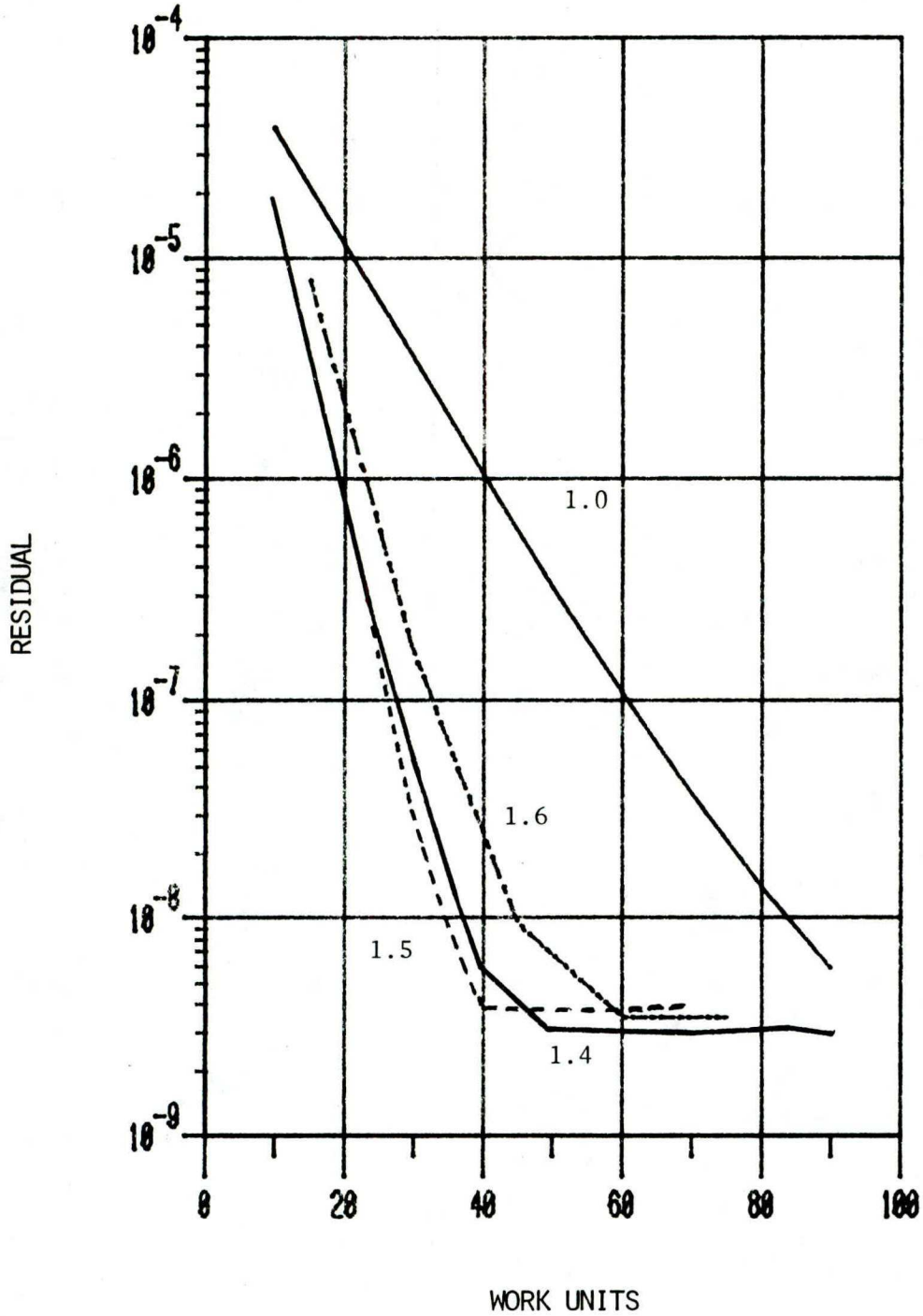

FIG. 6 OPTIMUM RELAXATION FACTOR FOR POINT SOR USING 17 X 33 NODES FOR CASCADE A.

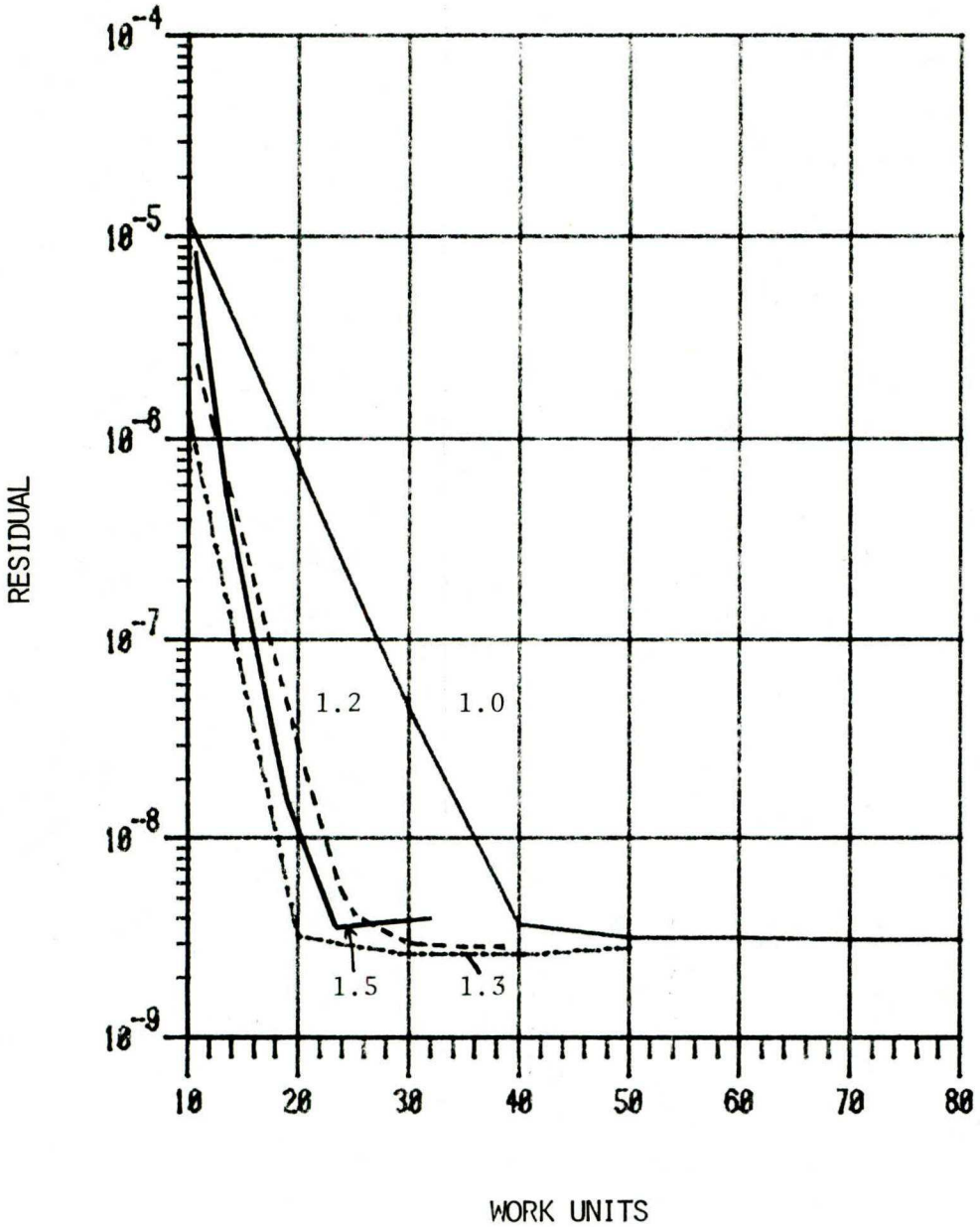

FIG. 7 OPTIMUM RELAXATION FACTOR FOR LINE SOR USING 17 X 33 NODES FOR CASCADE A.

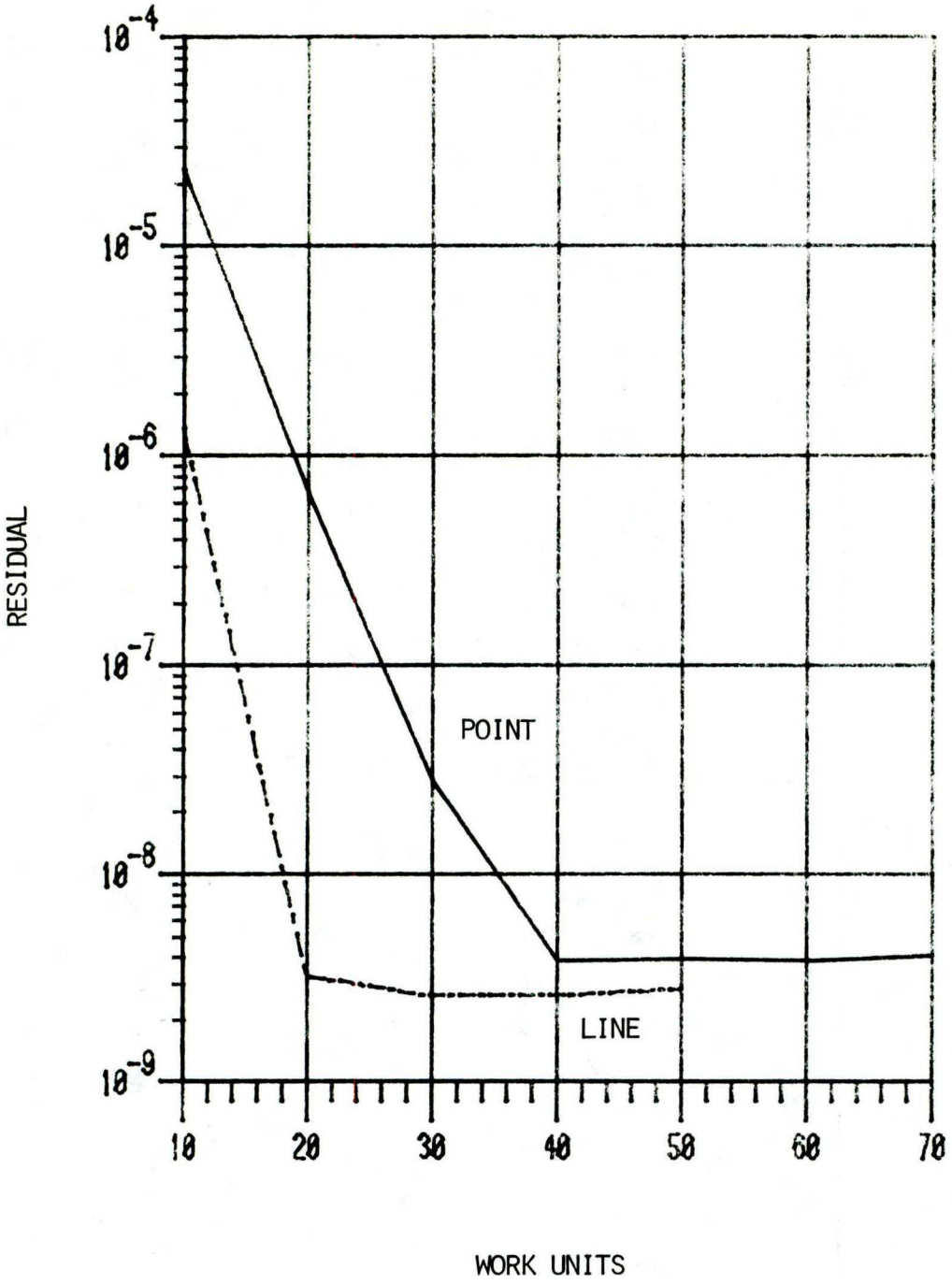

FIG. 8 COMPARISON OF OPTIMUM RELAXATIONS USING POINT AND LINE SOR FOR CASCADE A USING 17 X 33.

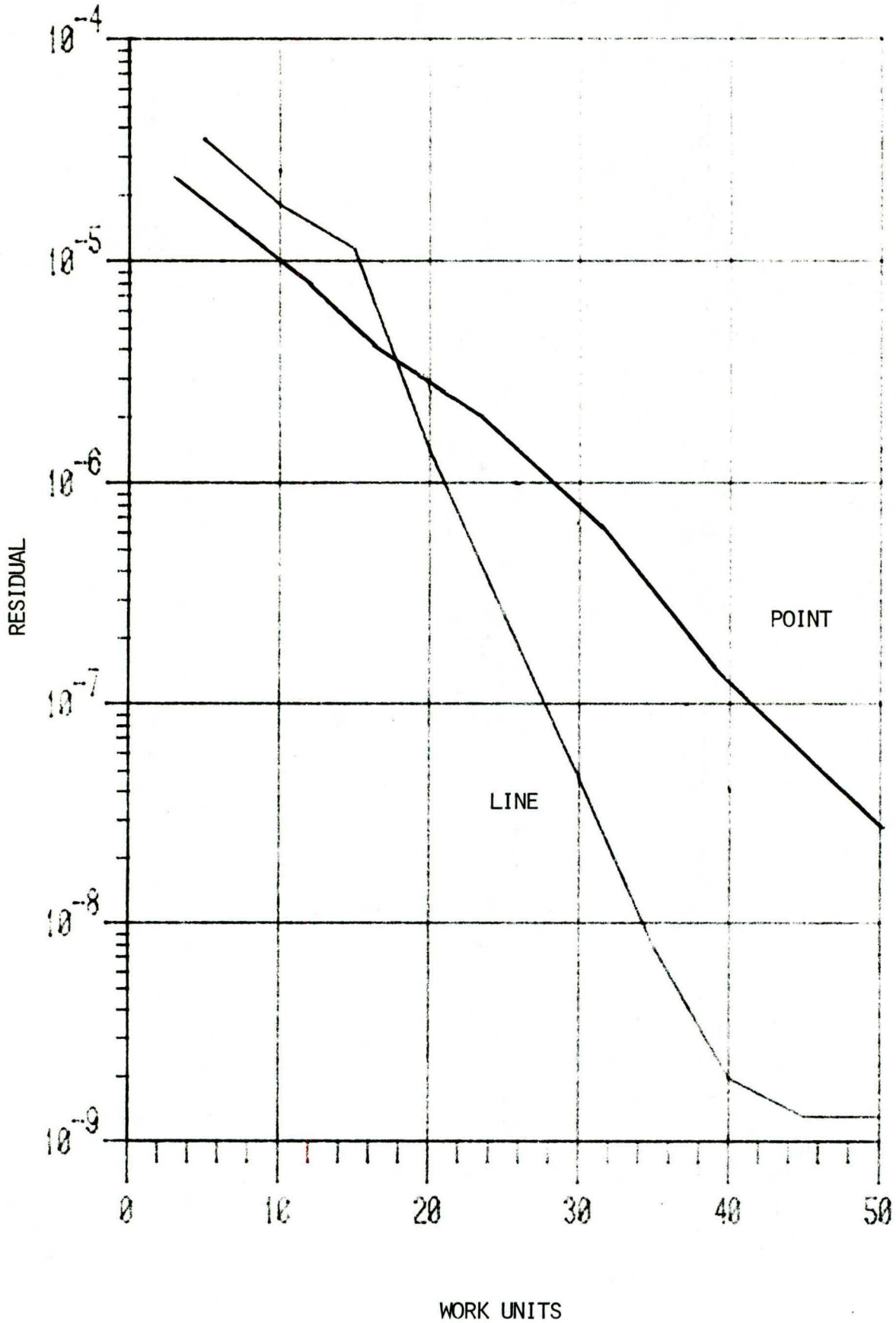

FIG. 9 COMPARISON OF OPTIMUM RELAXATIONS USING POINT AND LINE SOR FOR CASCADE B USING 17 X 33.

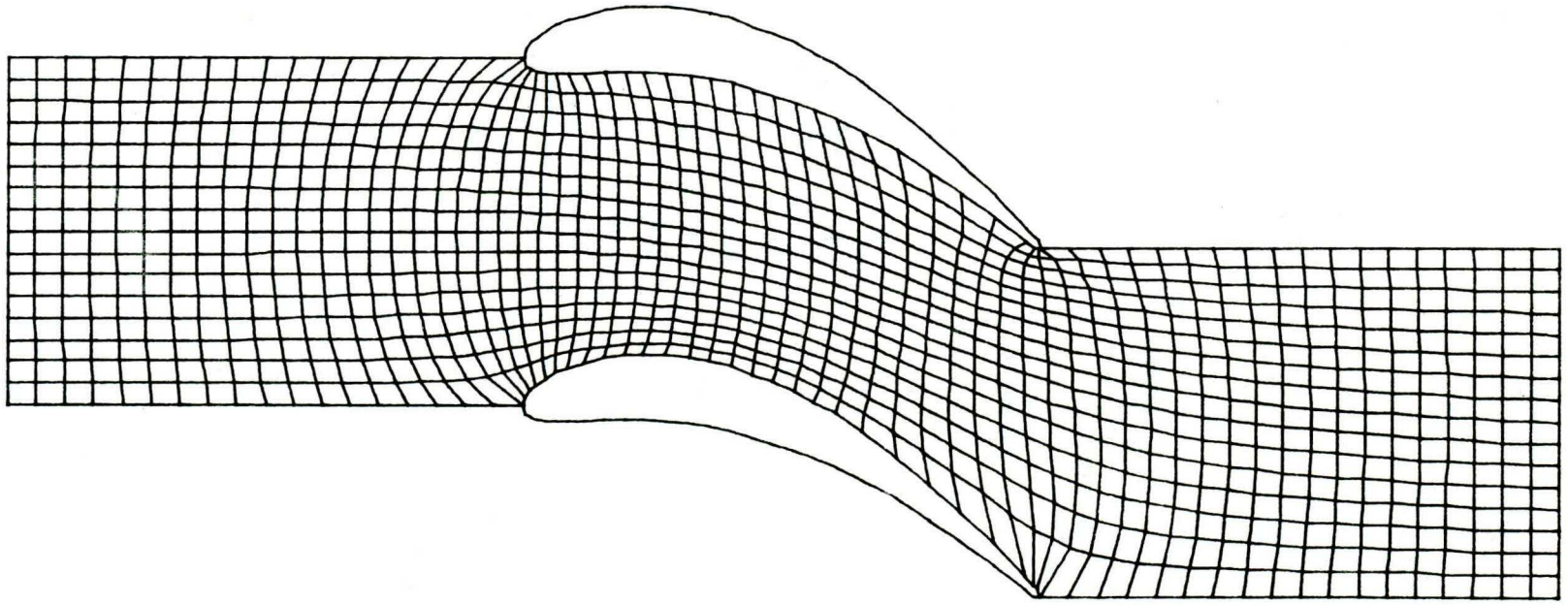

FIG. 10 BODY-FITTED COORDINATES FOR CASCADE A USING 17 X 65

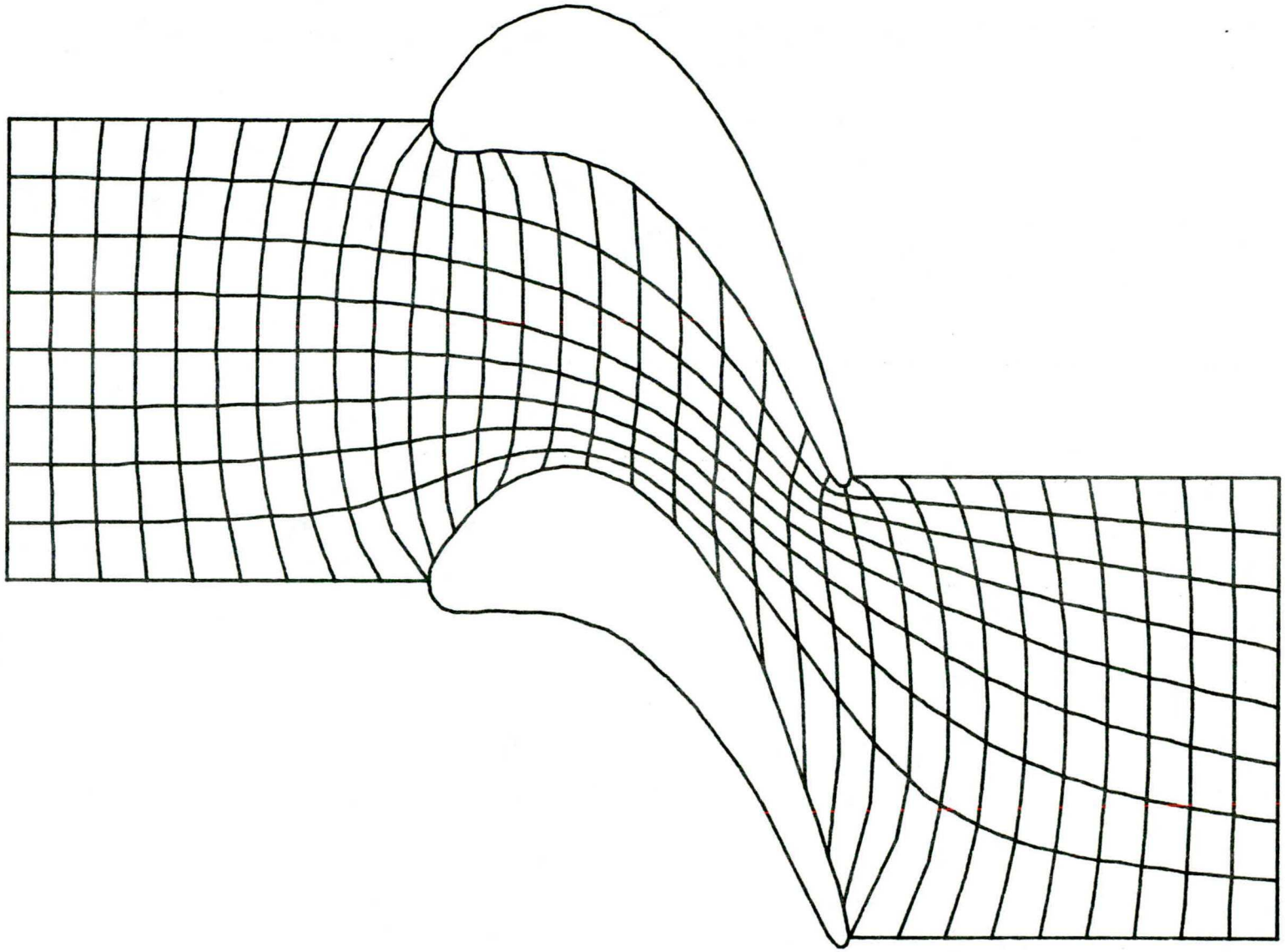

FIG. 11 BODY-FITTED COORDINATES FOR CASCADE B USING 17 x 65 (ONLY EVERY SECOND LINE IS DRAWN).

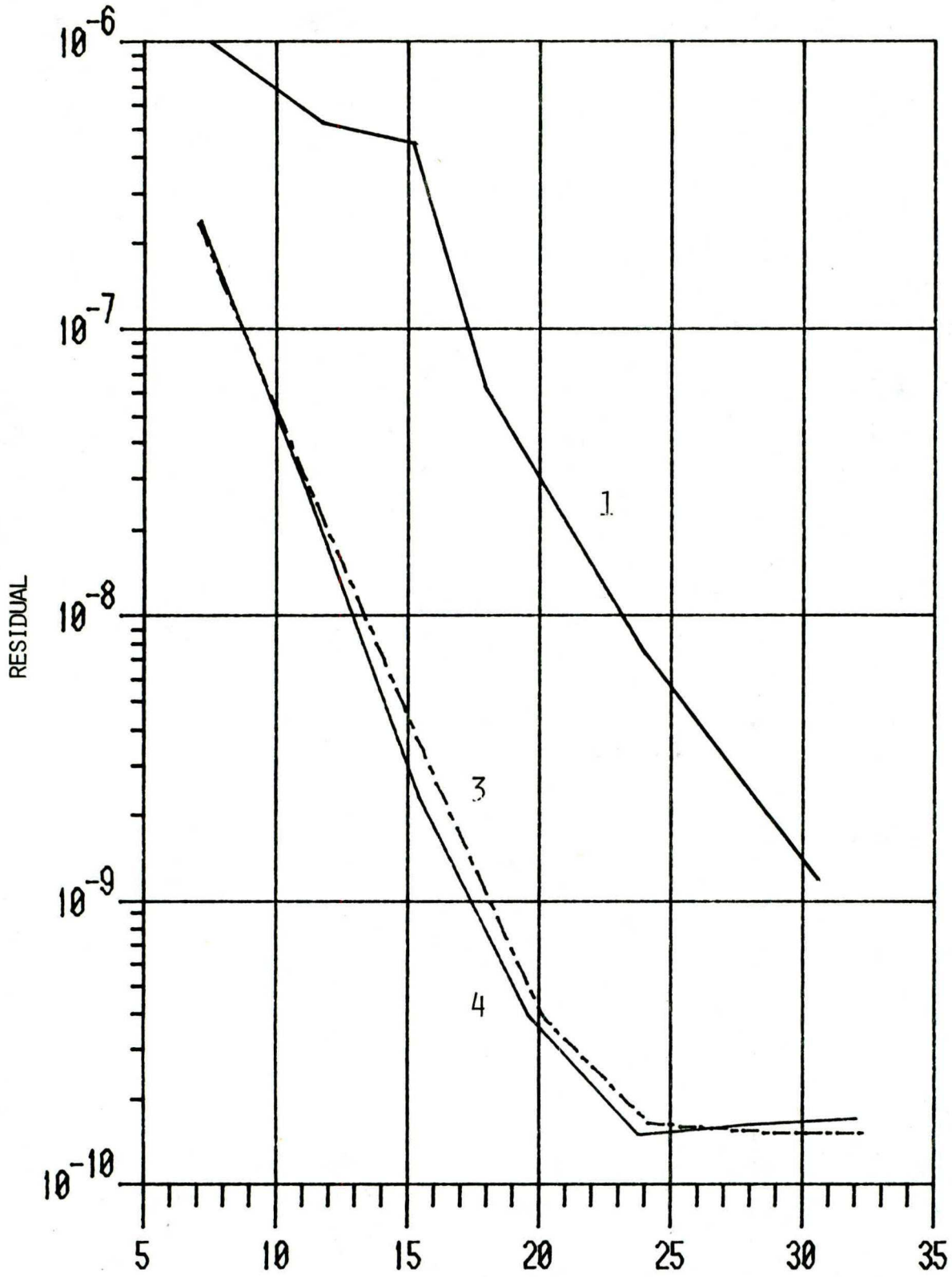

FIG. 12 COMPARISON OF RELAXATION HISTORIES USING 1, 3 AND 4 GRID LEVELS FOR LINE SOR AND MULTIGRID LINE SOR WITH THREE SWEEPS ON EACH LEVEL.

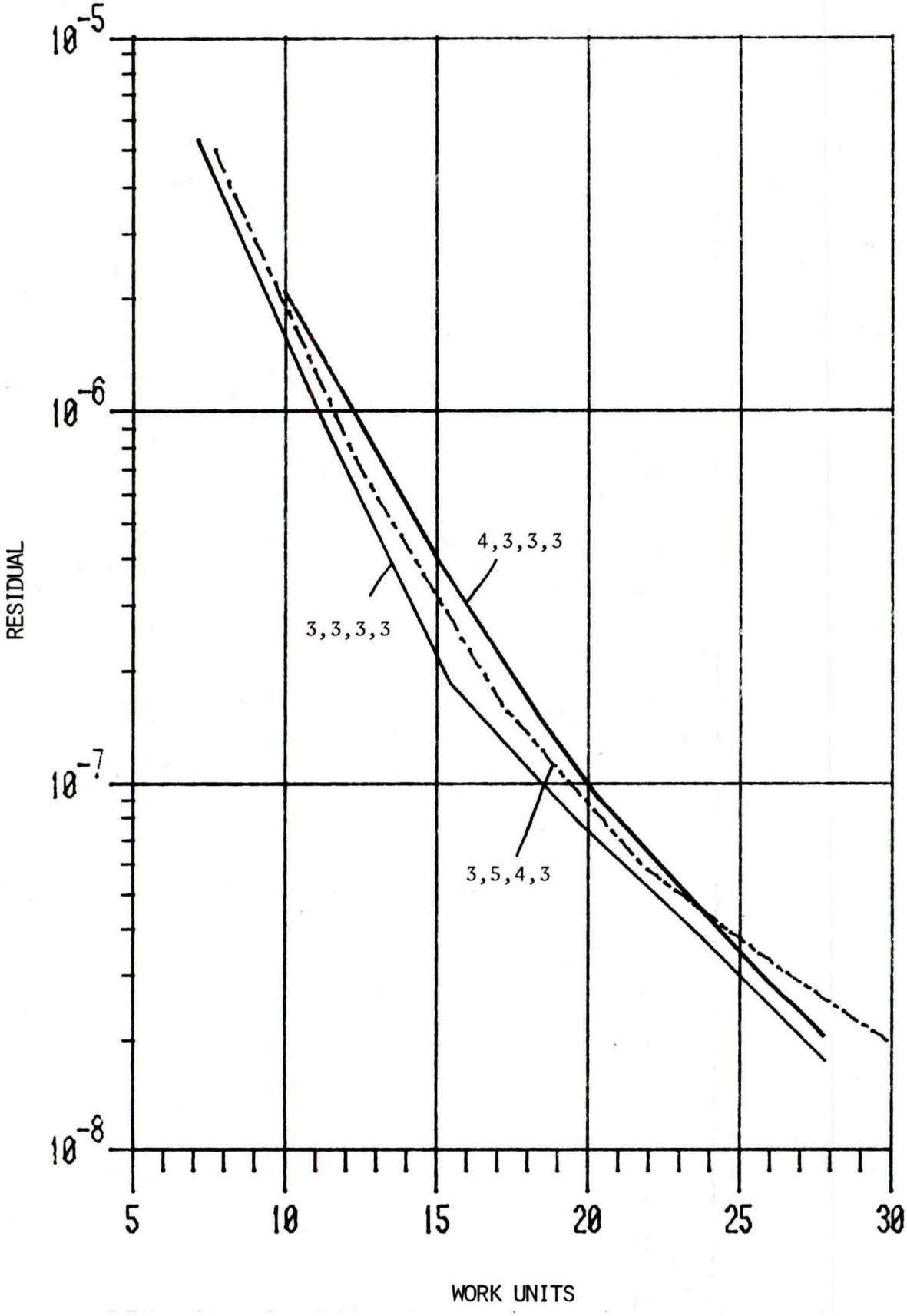

FIG. 13 COMPARISON OF RELAXATION HISTORIES OF MULTIGRID WITH POINT SOR USING 4 GRID LEVELS AND 3,3,3,3 AND 4,3,3,3 AND 3,5,4,3 SWEEPS ON THE FINE TO COARSE GRID.

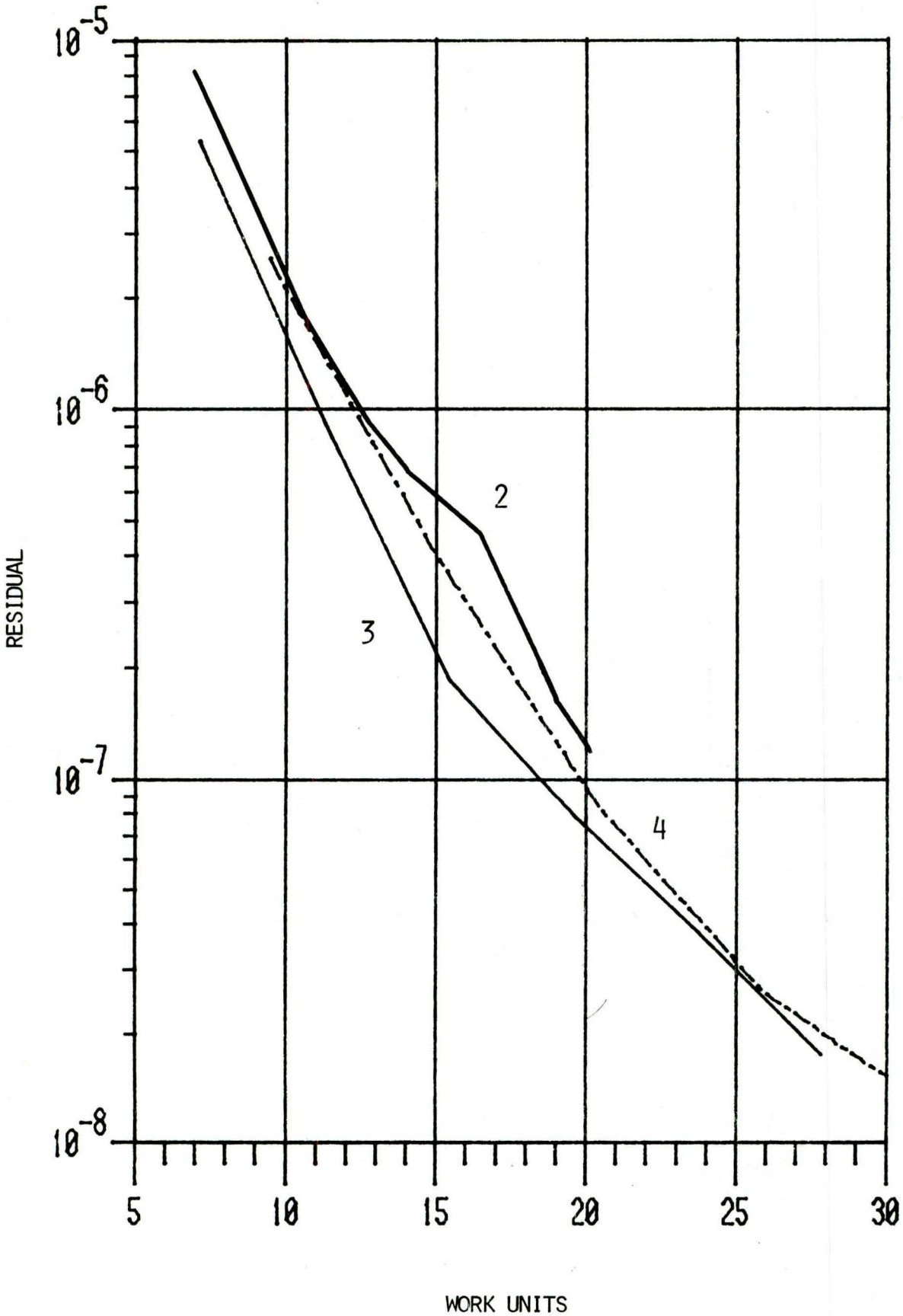

FIG. 14 OPTIMUM NUMBER OF SWEEPS PER LEVEL FOR MULTIGRID WITH POINT RELAXATION SHOWING RELAXATION HISTORIES WITH 2, 3 AND 4 SWEEPS PER LEVEL.

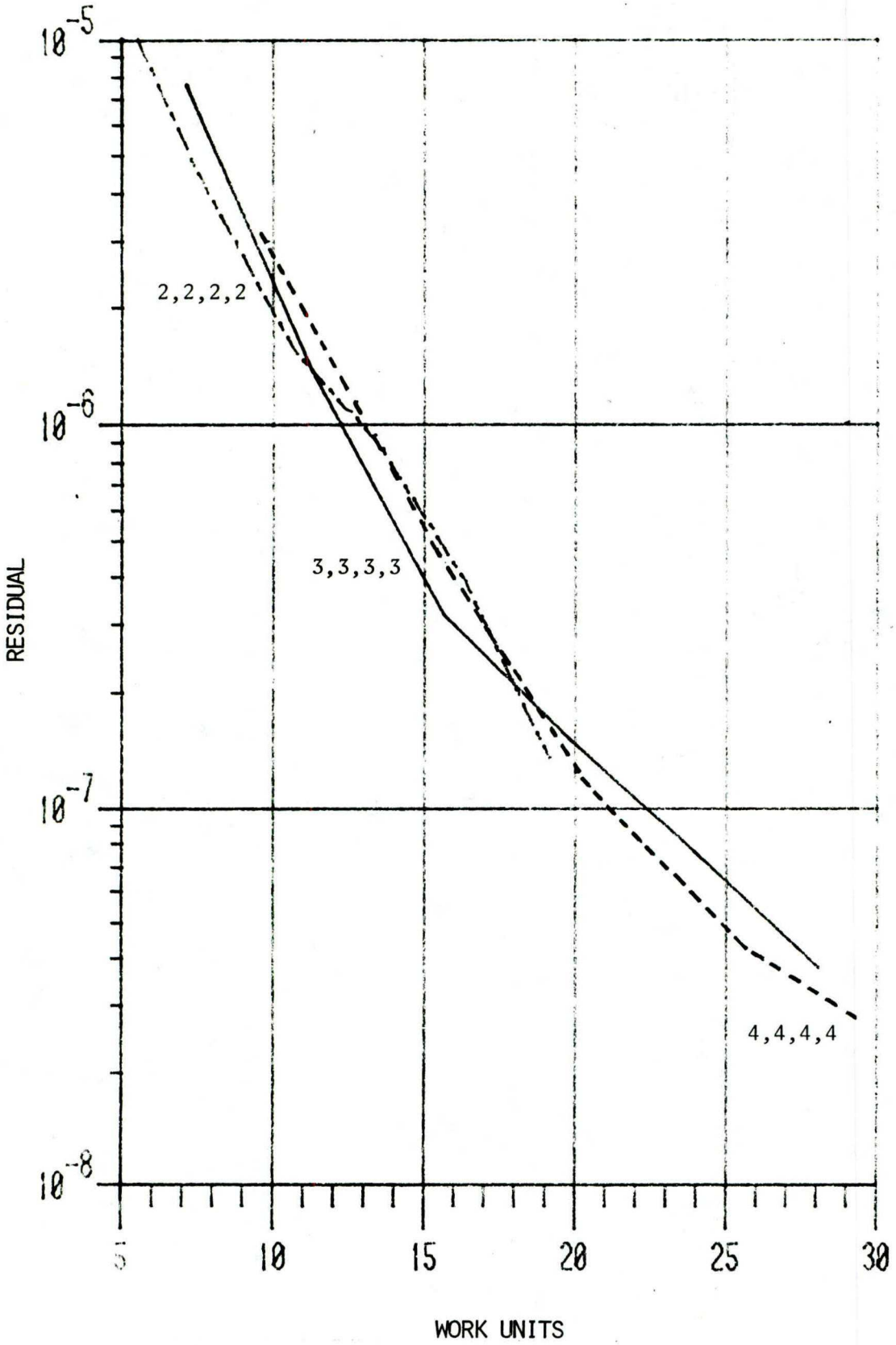

FIG. 15 OPTIMUM NUMBER OF SWEEPS PER LEVEL FOR MULTIGRID WITH LINE RELAXATION SHOWING RELAXATION HISTORIES WITH 3 AND 4 SWEEPS PER LEVEL.

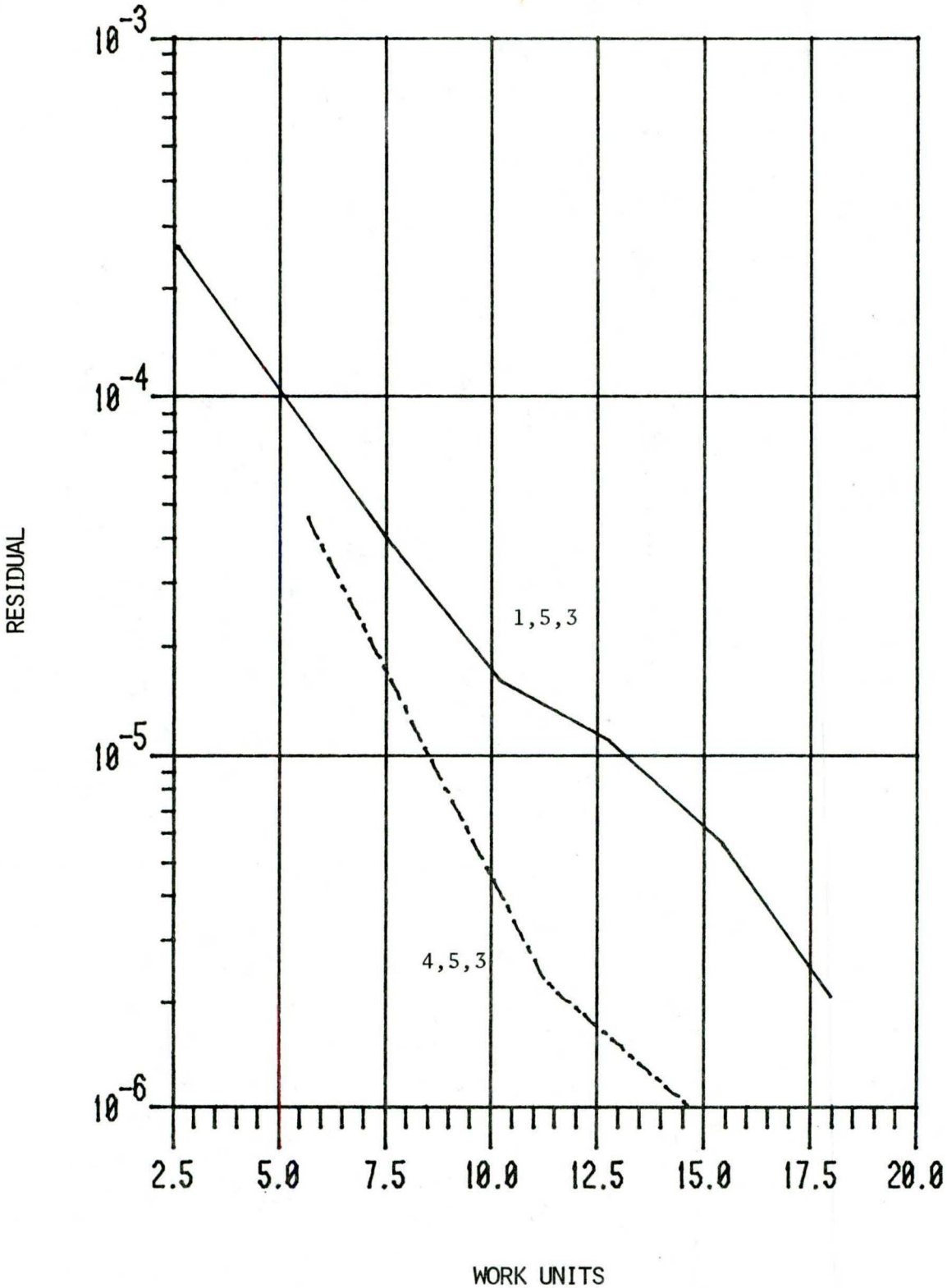

FIG. 16 EFFECT OF THE NUMBER OF SWEEPS ON THE FINE GRID ON THE CONVERGENCE RATE OF MULTIGRID WITH LINE RELAXATION.

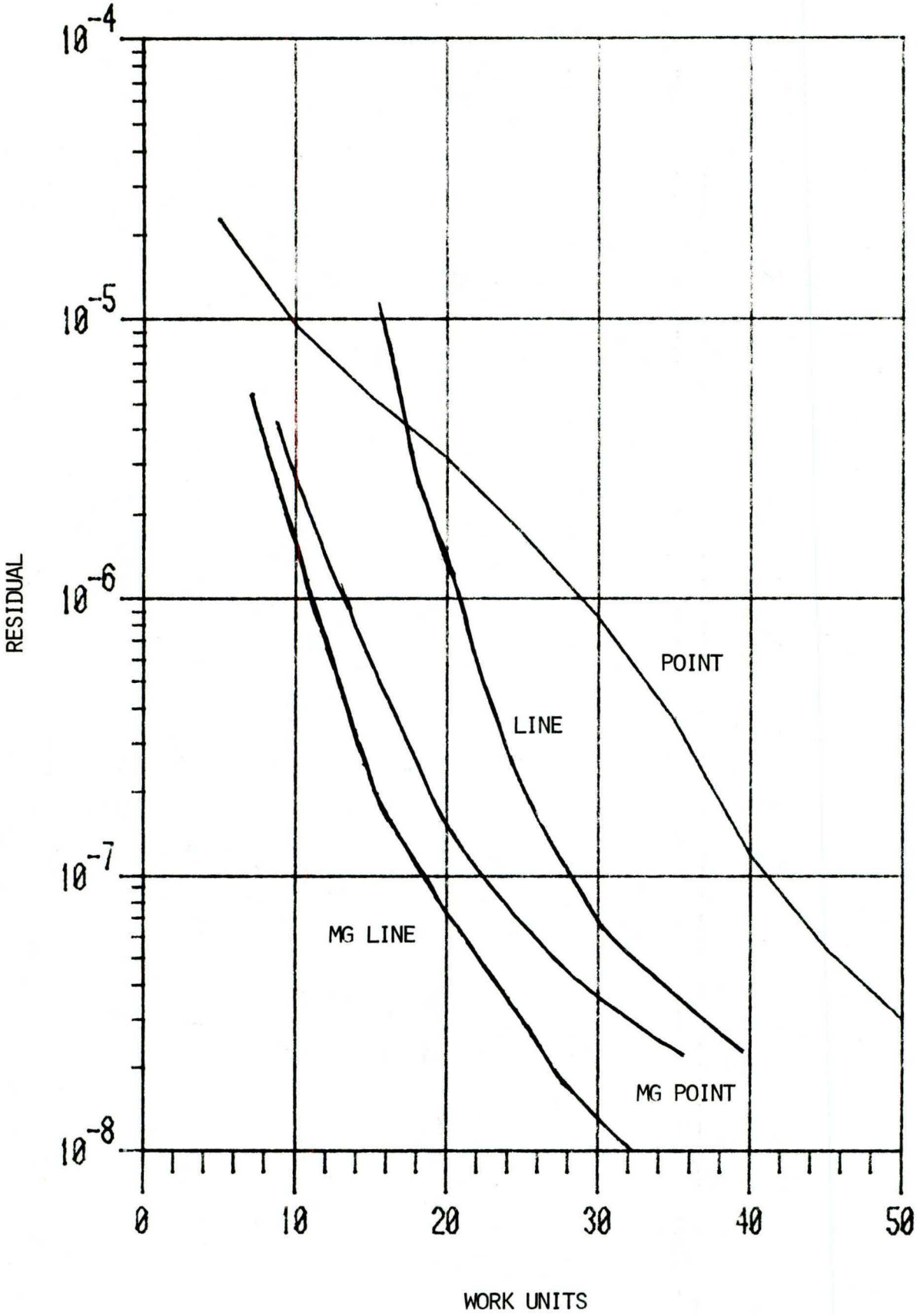

FIG. 17 COMPARISON OF RELAXATION HISTORIES FOR THE 4 METHODS FOR CASCADE A USING 9 x 17 NODES.

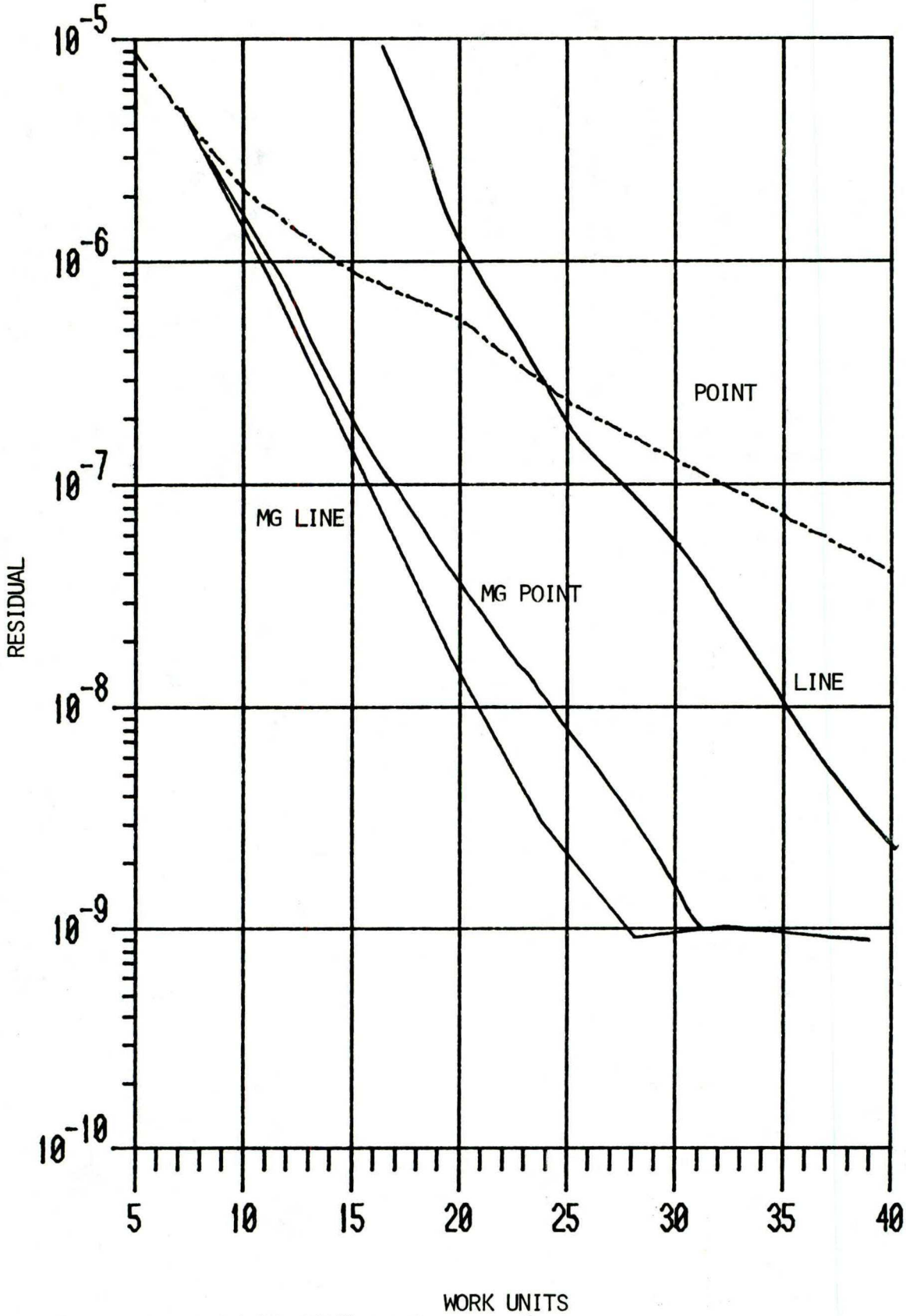

FIG. 18 COMPARISON OF RELAXATION HISTORIES FOR THE 4 METHODS FOR CASCADE A USING 17 x 33 NODES.

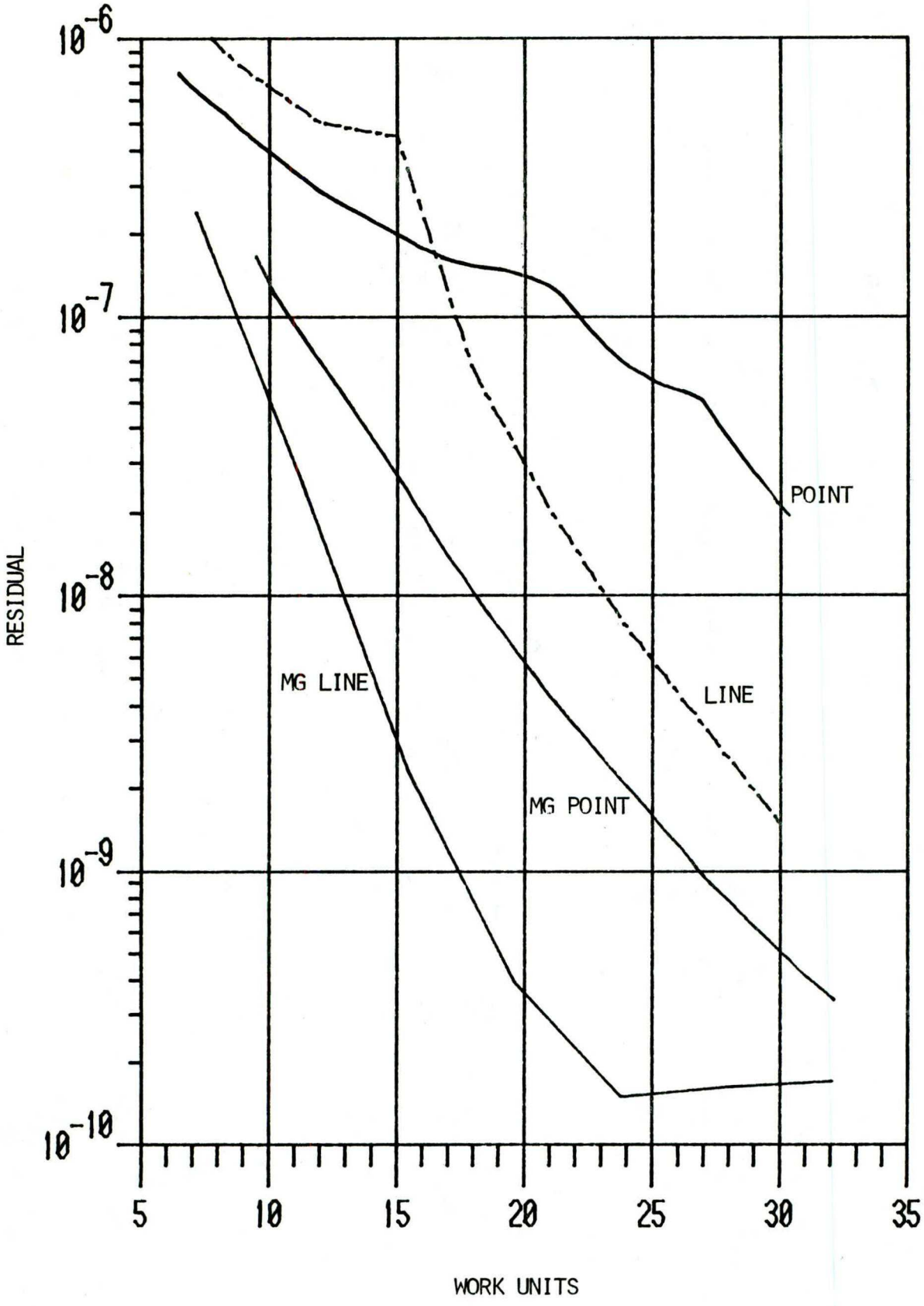

FIG. 19 COMPARISON OF RELAXATION HISTORIES FOR THE 4 METHODS FOR CASCADE A USING 17 x 65 NODES.

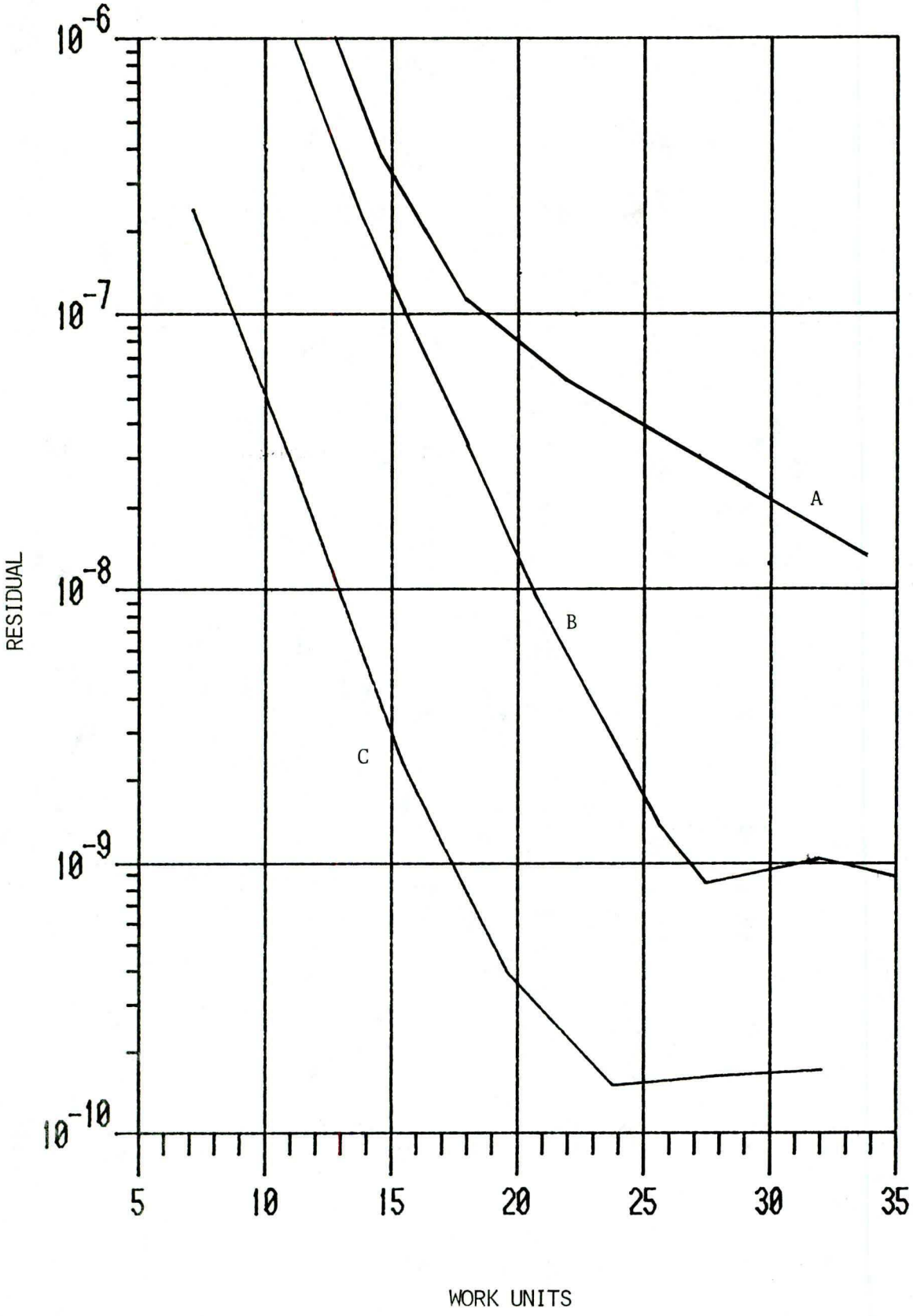

FIG. 20 EFFECT ON THE RELAXATION CONVERGENCE OF THE TOTAL NUMBER OF NODES, FOR 153(A), 561(B) AND 1105(C).

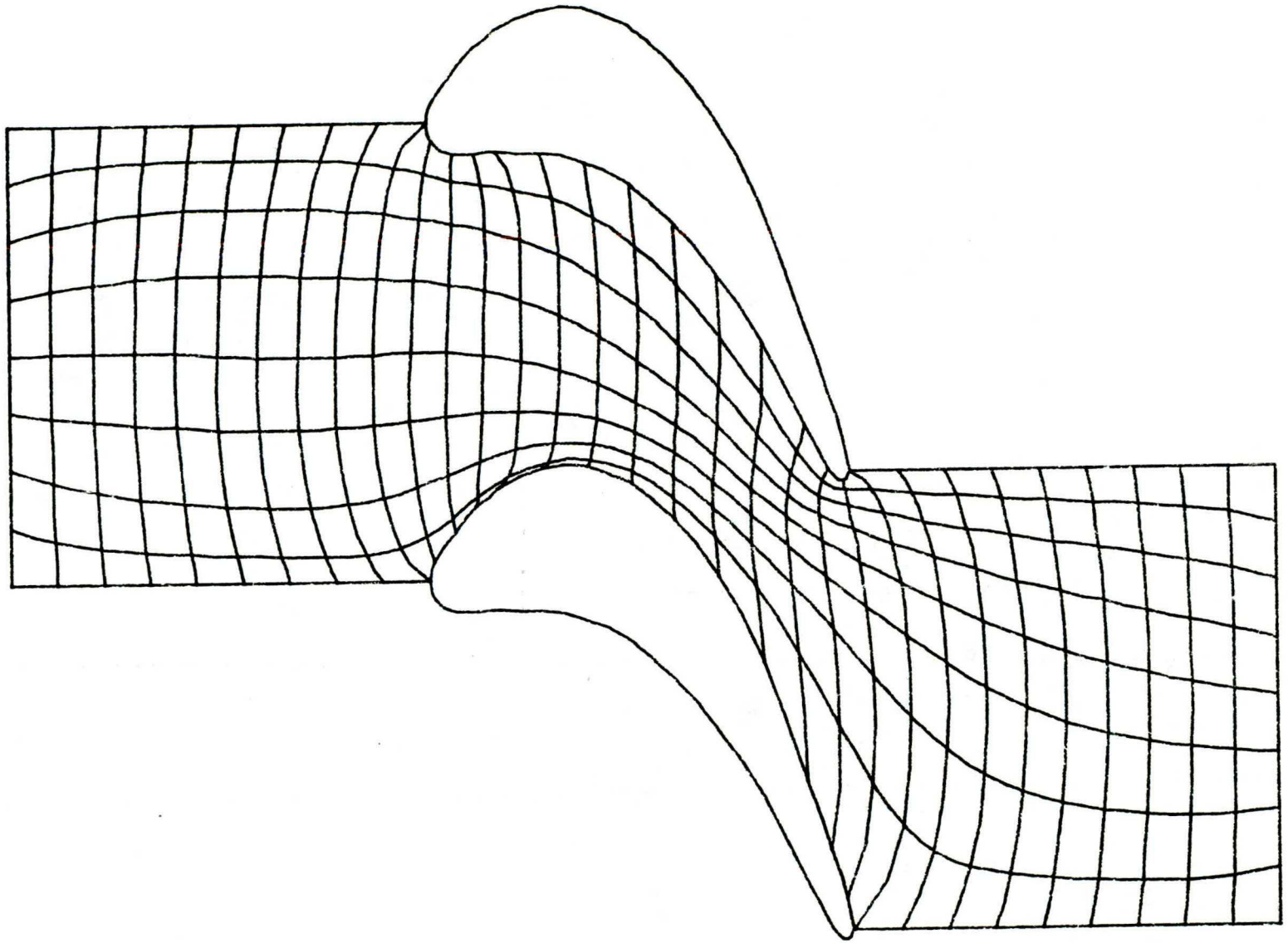

FIG. 21 ATTRACTION OF N-LINES TO THE TOP AND BOTTOM BOUNDARY FOR CASCADE B (17 x 65).

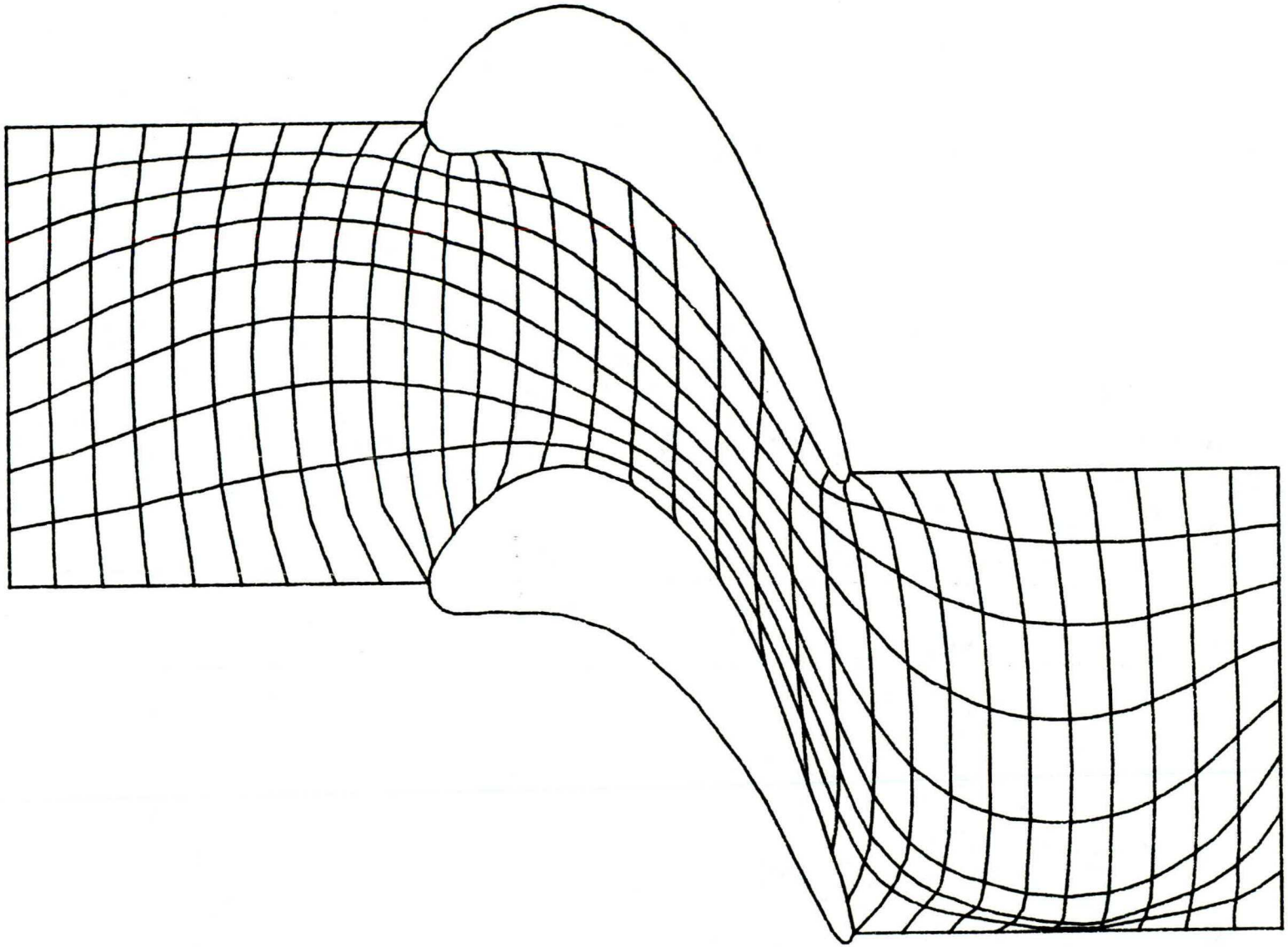

FIG. 22 ATTRACTION OF N-LINES TO TOP LEADING EDGE AND BOTTOM TRAILINGEDGE, FOR CASCADE B (17 x 65).

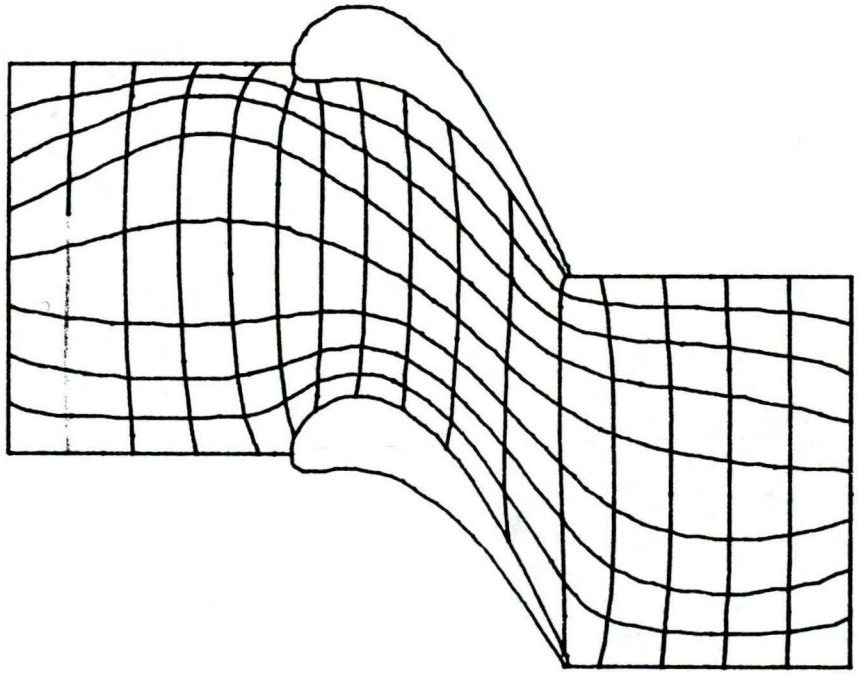

FIG. 23 ATTRACTION OF N-LINES TO TOP AND BOTTOM BOUNDARIES FOR CASCADE A.

ACKNOWLEDGEMENTS

This work was sponsored by the National Research Council of Canada and the Office of Research of Ecole Polytechnique.